BIFURCATION ANALYSIS OF A PREDATOR-PREY SYSTEM WITH NONMONOTONIC FUNCTIONAL RESPONSE*

HUAIPING ZHU[†], SUE ANN CAMPBELL[‡], AND GAIL S. K. WOLKOWICZ[†]

Abstract. We consider a predator-prey system with nonmonotonic functional response: $p(x) = \frac{mx}{ax^2+bx+1}$. By allowing b to be negative ($b > -2\sqrt{a}$), $p(x)$ is concave up for small values of $x > 0$ as it is for the sigmoidal functional response. We show that in this case there exists a Bogdanov–Takens bifurcation point of codimension 3, which acts as an organizing center for the system. We study the Hopf and homoclinic bifurcations and saddle-node bifurcation of limit cycles of the system. We also describe the bifurcation sequences in each subregion of parameter space as the death rate of the predator is varied. In contrast with the case $b \geq 0$, we prove that when $-2\sqrt{a} < b < 0$, a limit cycle can coexist with a homoclinic loop. The bifurcation sequences involving Hopf bifurcations, homoclinic bifurcations, as well as the saddle-node bifurcations of limit cycles are determined using information from the complete study of the Bogdanov–Takens bifurcation point of codimension 3 and the geometry of the system. Examples of the predicted bifurcation curves are also generated numerically using XPPAUT. Our work extends the results in [F. Rothe and D. S. Shafer, *Proc. Roy. Soc. Edinburgh Sect. A*, 120 (1992), pp. 313–347] and [S. Ruan and D. Xiao, *SIAM J. Appl. Math.*, 61 (2001), pp. 1445–1472].

Key words. predator-prey system, Hopf bifurcation, homoclinic bifurcation, Bogdanov–Takens bifurcation, saddle-node bifurcation of limit cycles, limit cycle

AMS subject classifications. Primary, 34C25, 92D25; Secondary, 58F14

PII. S0036139901397285

1. Introduction. The classical predator prey model with an inhibition response function was introduced in Freedman and Wolkowicz [12] to establish a veritable paradox of enrichment. In this paper we analyze the classical predator-prey model with a specific inhibition response function, the Holling type IV response function. In particular, we study the model

$$
(1.1) \quad
\begin{cases}
\dot{x} & = rx\left(1 - \dfrac{x}{K}\right) - yp(x) = p(x)(F(x) - y), \\[2mm]
\dot{y} & = y(-d + cp(x)), \\[1mm]
& x(0) \geq 0, y(0) \geq 0,
\end{cases}
$$

where x and y denote the density of the prey and predator populations, respectively, r, K, d, and c are positive constants, and $F(x) = rx(1 - \frac{x}{K})/p(x)$.

The specific growth rate of the prey population in the absence of predator population is assumed to satisfy logistic growth, and so r denotes the intrinsic growth rate of the prey population, and K denotes the carrying capacity. The natural death rate of the predators is denoted by d, and the predator response function is denoted by $p(x)$. It is assumed that the rate of conversion of prey captured to predator is proportional

†Department of Mathematics and Statistics, McMaster University, Hamilton, Ontario, Canada L8S 4K1 (hzhu@icarus.math.mcmaster.ca, wolkowic@icarus.math.mcmaster.ca).

‡Department of Applied Mathematics, University of Waterloo, Waterloo, Ontario, Canada N2L 3G1 and Centre for Nonlinear Dynamics in Physiology and Medicine, McGill University, Montreal, Quebec, Canada H3G 1Y6 (sacampbe@duchatelet.math.uwaterloo.ca).

to the predator response function, where c is the constant of proportionality or yield constant.

The predator-prey system (1.1) has been extensively studied by many authors. (See Ruan and Xiao [28] and Wolkowicz [30] for an extended list of references.) In the literature, different functions have been used to model the predator response. (See Holling [15] and Freedman and Wolkowicz [12] for a description of the general conditions that this function should satisfy.) In Wolkowicz [30], assuming only these general conditions and a technical assumption, a complete one parameter bifurcation analysis of (1.1) was carried out using the carrying capacity K as the bifurcation parameter. It was proved that the model has rich dynamics, including parameters for which there is a homoclinic bifurcation. It was pointed out that both supercritical and subcritical Hopf bifurcations are possible, and that when there is a subcritical Hopf bifurcation, there must be parameters for which there is a saddle-node bifurcation of limit cycles and a range of parameters for which there are at least two limit cycles. To do a more detailed analysis, it is useful to specify the function $p(x)$.

The form most often used (see, for example, Holling [14]), is the Holling type II form, $p(x) = \frac{mx}{b+x}$, also associated with Monod and Michaelis–Menten. This is an increasing function that saturates, i.e., has a finite positive limit as x approaches infinity. For a very nice description of the biological interpretation of each of the parameters, see Rinaldi, Muratori, and Kuznetsov [24], where they also study the effect of periodically forcing each of the parameters individually, and propose a universal bifurcation diagram.

In this paper we consider the Holling type IV functional response, associated with Monod–Haldane (see Andrews [1]):

$$(1.2) \qquad p(x) = \frac{mx}{ax^2 + bx + 1},$$

where a and m are positive constants, and $b > -2\sqrt{a}$ (so that $ax^2 + bx + 1 > 0$ for all $x \geq 0$ and hence $p(x) > 0$ for all $x > 0$).

When a is positive, this function increases to a maximum and then decreases, approaching zero as x approaches infinity. Thus, $p(x)$ models the situation where the prey can better defend or disguise themselves when their population becomes large enough, a phenomenon called group defense. See [12] and [28] for more information about this phenomenon and examples of populations that use this strategy.

The response function (1.2) has been primarily considered assuming m positive and a and b nonnegative. In this case, for x sufficiently small, $p(x)$ resembles the Holling type II model while for large x the effect of inhibition is seen (Figure 1.1(a)). If $-2\sqrt{a} < b < 0$ and a is nonnegative, $p(x)$ remains nonnegative, the inhibition effect is still observed for large x, however, for x small $p(x)$ resembles the Holling type III (sigmoidal) function (Figure 1.1(b)). We shall show in section 5 that for model (1.1) with the nonmonotonic response function (1.2), the organizing center of the bifurcation diagram is at

$$b = -\sqrt{a}, \qquad d = \frac{mc}{b + 2\sqrt{a}}, \qquad K = \frac{2}{\sqrt{a}},$$

where there is a Bogdanov–Takens bifurcation of codimension 3. Ignoring the negative, but physically relevant, values of b misses this important fact as well as some rich dynamics of the model.
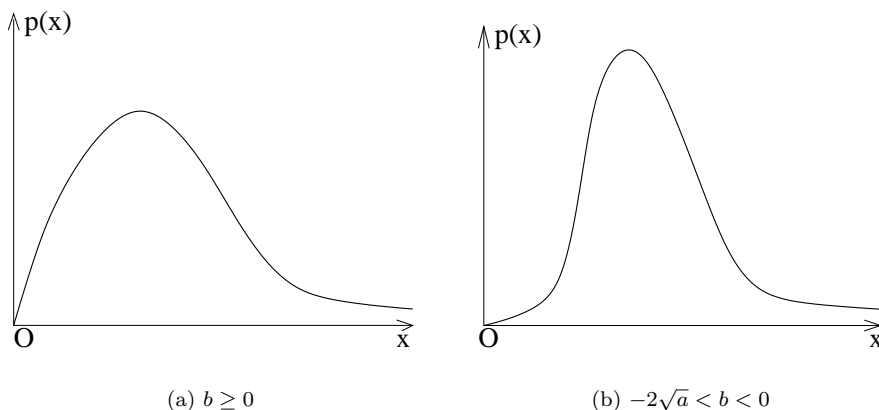
(a) $b \geq 0$ (b) $-2\sqrt{a} < b < 0$

FIG. 1.1. *Response functions.*

Using the response function (1.2) in (1.1), the model to be considered is

$$
(1.3) \quad
\begin{cases}
\dot{x} &= rx\left(1 - \dfrac{x}{K}\right) - y\dfrac{mx}{ax^2 + bx + 1} = p(x)(F(x) - y), \\[2mm]
\dot{y} &= y\left(-d + c\dfrac{mx}{ax^2 + bx + 1}\right) = y(-d + cp(x)), \\[2mm]
x(0) &\geq 0, y(0) \geq 0,
\end{cases}
$$

where

$$
(1.4) \qquad F(x) = \frac{r}{m}\left(1 - \frac{x}{K}\right)(ax^2 + bx + 1)
$$

and

$$
(1.5) \qquad K, \ r, \ m, \ a, \ c, \ d > 0, \quad \text{and} \quad b > -2\sqrt{a}.
$$

Rothe and Shafer [25, 26] considered the system

$$
(1.6) \quad
\begin{cases}
\dfrac{dx}{d\tau} &= rx\left[\left(1 - \dfrac{x}{K}\right)\left(\left(\dfrac{x}{\lambda} - 1\right)\left(\dfrac{x}{\mu} - 1\right) + x\right) - y\right], \\[2mm]
\dfrac{dy}{d\tau} &= -y\left(\dfrac{x}{\lambda} - 1\right)\left(\dfrac{x}{\mu} - 1\right),
\end{cases}
$$

which may be obtained from (1.3) by rescaling time t via

$$
\tau = \int_0^t \left[\frac{1}{ax^2(t) + bx(t) + 1}\right] dt
$$

and by assuming that the system always has two equilibria inside the positive quadrant. Using results for polynomial systems and taking $(\frac{1}{K}, \frac{1}{\lambda}, \frac{1}{\mu})$ as parameters, the authors studied the bifurcations of the model. Rothe and Shafer were the first to consider the case b negative $(-2\sqrt{a} < b)$. However, after the transformation and reduction to (1.6), the effect of allowing $b < 0$ was hidden. They proved that there is a set of parameters for which there is a cusp of codimension 2, in a neighborhood of

which the system realizes every phase portrait possible under small smooth perturbation. They also indicated that there is a cusp of codimension at least 3, but did not prove that the codimension is exactly 3. They point out for parameters near this cusp there is a semi-stable limit cycle. The results of [26] are in terms of parameters which are composites of the model parameters and thus are more difficult to interpret for the biological system.

In [28], Ruan and Xiao restricted $b = 0$ in (1.3) and carried out a global analysis. In particular, they proved that a limit cycle cannot coexist with a homoclinic loop. They determined a set of parameters for which the system has a unique limit cycle which is stable and another for which no cycles exist. They also studied the Bogdanov–Takens bifurcation of codimension 2.

Model (1.3) involves 7 parameters (see (1.5)) that all have biological interpretations. By rescaling the state variables and time we could eliminate 3 of them. For example, we could eliminate a, m, and c by using

$$(1.7) \qquad (t,\ x,\ y) \longrightarrow \left(\frac{\sqrt{a}}{mc}t,\ \frac{1}{\sqrt{a}}x,\ \frac{c}{\sqrt{a}}y \right)$$

and replacing r by $\frac{\sqrt{a}}{mc}r$, K by $\sqrt{a}K$, d by $\frac{\sqrt{a}}{mc}d$, and b by $\frac{1}{\sqrt{a}}b$. Similarly, using the change of variables

$$(t,\ x,\ y) \longrightarrow \left(\frac{t}{r},\ \frac{r}{mc}x,\ \frac{r}{m}y \right),$$

and replacing a by $(\frac{r}{mc})^2 a$, K by $\frac{mc}{r}K$, d by $\frac{1}{r}d$, and b by $\frac{r}{mc}b$ we could eliminate r, m, and c. We choose not to do this so that the effect of all the parameters may be easily seen in our results.

The x and y axes, the nonnegative cone and its interior are all invariant sets with respect to system (1.3). A standard phase plane argument can be used to show that all solutions initiating in the positive cone are bounded (see [30]).

This paper is organized as follows. Section 2 contains the linear analysis of the equilibria, where we emphasize how this depends on the slope of the prey isocline. In section 3 we give the geometric properties of the predator and prey isoclines, and we show how the parameters (1.5) influence the geometry of the isoclines. In section 4, we study the effect of this geometry on the existence, number, and criticality of Hopf bifurcations which occur as $\hat{d} = \frac{d}{mc}$ is varied. We determine that the parameter r plays no role here. In section 5, we continue our analysis, examining the degenerate equilibria, especially the cusp points of codimension 2 and 3. In section 6 we consider the global dynamics. We conclude with section 7 where we summarize our results, compare them with other closely related results, and indicate their biological significance.

2. Linear stability analysis. We consider equilibrium solutions to exist only if they lie in the nonnegative cone. System (1.3) has at most four equilibrium solutions. Two always lie on the boundary of the nonnegative cone: $E_0 = (0, 0)$, representing the extinction of both species, and $E_K = (K, 0)$, representing the extinction of the predator population and the density of the prey population equilibrating at the carrying capacity.

Let $\lambda \leq \mu$ denote the two possible solutions of the quadratic equation $cp(x) = d$, and $E_\lambda = (\lambda, F(\lambda))$ and $E_\mu = (\mu, F(\mu))$ denote the corresponding equilibria. Whether zero, one, or both of these other equilibria exist and sit in the nonnegative cone
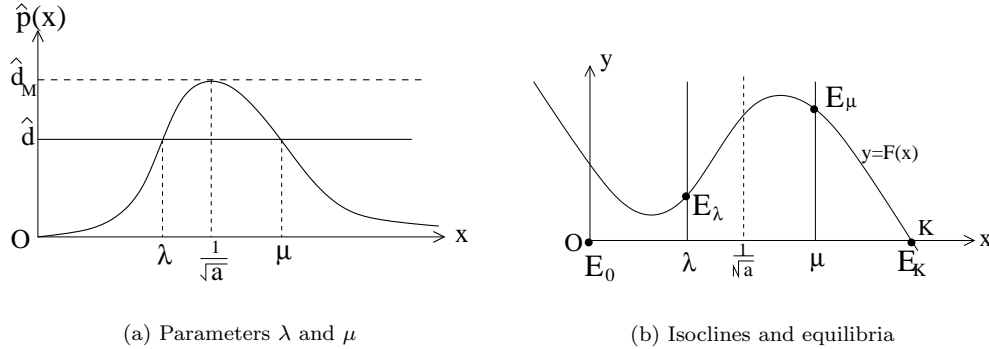
(a) Parameters λ and μ (b) Isoclines and equilibria

FIG. 2.1. *Typical geometry for system* (1.3).

depends on the relative positions of the prey isocline $y = F(x)$ and the predator isoclines $x = \lambda$ and $x = \mu$. Figure 2.1(b) illustrates one of the possible positions, where both E_λ and E_μ exist.

Define

$$\hat{d} = \frac{d}{mc},$$

(2.1)

$$\hat{p}(x) = \frac{p(x)}{m}.$$

Then $cp(x) = d$ or $\hat{p}(x) = \hat{d}$ is equivalent to

(2.2) $$\hat{g}(x) = a\hat{d}x^2 - (1 - b\hat{d})x + \hat{d} = 0.$$

If we define

(2.3) $$\hat{d}_M = \frac{1}{b + 2\sqrt{a}},$$

$$\Delta_0 = (1 - b\hat{d})^2 - 4a\hat{d}^2,$$

then from a simple calculation it follows that for $\hat{d} \in (0, \hat{d}_M]$, (2.2) has two positive roots $\lambda \leq \mu$ where

(2.4) $$\lambda := \frac{1 - b\hat{d} - \sqrt{\Delta_0}}{2a\hat{d}}, \quad \mu := \frac{1 - b\hat{d} + \sqrt{\Delta_0}}{2a\hat{d}}.$$

If $\hat{d} \in (0, \hat{d}_M)$, then $\lambda < \frac{1}{\sqrt{a}} < \mu$. As $\hat{d}$ increases, λ increases and μ decreases. When $\hat{d} = \hat{d}_M$, $\lambda = \mu = \frac{1}{\sqrt{a}}$ (Figure 2.1(a)). When $\hat{d} > \hat{d}_M$, λ and μ are no longer real. Then E_0 and E_K are the only equilibria in the nonnegative cone, and E_K attracts all orbits initiating in the positive cone.

Next we investigate the stability of the equilibrium solutions E_0, E_K, E_λ, and E_μ by linearizing about each one. The variational matrix about any equilibrium $(\bar{x}, \bar{y})$ is

(2.5) $$V(\bar{x}, \bar{y}) = \begin{bmatrix} p'(\bar{x})(F(\bar{x}) - \bar{y}) + p(\bar{x})F'(\bar{x}) & -p(\bar{x}) \\ cp'(\bar{x})\bar{y} & cp(\bar{x}) - d \end{bmatrix}.$$

TABLE 2.1
Linear analysis of the equilibrium solutions.

Fixed point	$K < \lambda < \mu$	$\lambda < K < \mu$	$\lambda < \mu < K$	
E_0	saddle	saddle	saddle	
E_K	attracting node	saddle	attracting node	
E_λ	does not exist	repeller	repeller	$F'(\lambda) > 0$
		attractor	attractor	$F'(\lambda) < 0$
E_μ	does not exist	does not exist	saddle	

An easy calculation indicates that E_0 is always a saddle point. For E_μ, note that the determinant of $V(\mu, F(\mu))$ is

$$(2.6) \qquad \det\Big(V(\mu, F(\mu))\Big) = c\bar{y}p(\mu)p'(\mu) = \frac{c\hat{d}m^2 F(\mu)(1 - a\mu^2)}{(a\mu^2 + b\mu + 1)^2},$$

and that for $\hat{d} \in (0, \hat{d}_M)$, $\mu > \frac{1}{\sqrt{a}}$. Hence, if E_μ lies in the positive cone, i.e., when $\mu < K$, $\det(V(\mu, F(\mu))) < 0$, therefore E_μ is a saddle point.

Similarly, when E_λ lies in the positive cone, i.e., if $\lambda < K$, $\det(V(\lambda, F(\lambda))) > 0$. Further, the trace of $V(\lambda, F(\lambda))$ is

$$(2.7) \qquad\qquad\qquad \operatorname{tr} V(\lambda, F(\lambda)) = p(\lambda)F'(\lambda).$$

Hence, E_λ is an attractor (resp., repeller) if $F'(\lambda) < 0$ (resp., $F'(\lambda) > 0$).

From the discussion above, it is clear that there is a saddle-node bifurcation involving E_λ and E_μ when $\hat{d} = \hat{d}_M$.

The two eigenvalues of the variational matrix about E_K are $-r < 0$ and $-d + cp(K) = mc[\hat{p}(K) - \hat{d}]$. Thus E_K is an attracting node if $\hat{d} > \hat{p}(K)$. It is a saddle point if $\hat{d} < \hat{p}(K)$. If $\hat{d} = \hat{p}(K)$, E_K undergoes a transcritical bifurcation. As $\hat{d}$ increases from 0, the steady state bifurcations outlined below occur.

1. If $K < \frac{1}{\sqrt{a}}$, denote $\hat{d}_{\lambda K} = \hat{p}(K)$. A transcritical bifurcation involving E_λ and E_K occurs when $\hat{d} = \hat{d}_{\lambda K}$. E_K changes its stability from a saddle point to an attracting node. When $\hat{d} = \hat{d}_M$, a saddle-node bifurcation involving E_λ and E_μ occurs outside the nonnegative cone.

2. If $K > \frac{1}{\sqrt{a}}$, denote $\hat{d}_{\mu K} = \hat{p}(K)$. A transcritical bifurcation involving E_μ and E_K occurs when $\hat{d} = \hat{d}_{\mu K}$. E_K changes its stability from a saddle point to an attracting node. When $\hat{d} = \hat{d}_M$, a saddle-node bifurcation involving E_λ and E_μ occurs inside the positive cone.

3. If $K = \frac{1}{\sqrt{a}}$, then $\hat{p}(K) = \hat{d}_M$. When $\hat{d} = \hat{d}_M$, E_λ, E_μ, and E_K coalesce at E_K. Phase portrait analysis shows that E_K is an asymptotically stable degenerate node.

The linear analysis for system (1.1) is summarized in Table 2.1.

3. Geometry of the isoclines. The geometry of the prey and predator isoclines plays an important role in the analysis of both the local and global bifurcations. We begin with a useful observation about the intersections of the prey isocline $y = F(x)$ with the predator isoclines, the lines $x = \lambda$ and $x = \mu$.

LEMMA 3.1. *Consider $F(\lambda)$ and $F(\mu)$:*

1. If $0 < K < \frac{2}{\sqrt{a}}$ and $\hat{d} \in (0, \hat{d}_M)$, then $F(\lambda) > F(\mu)$.
2. If $K = \frac{2}{\sqrt{a}}$, then $F(\lambda) = F(\mu)$ if and only if $\hat{d} = \hat{d}_M$. *Otherwise, if $\hat{d} \in$*
    $(0, \hat{d}_M)$, then $F(\lambda) > F(\mu)$.
3. If $K > \frac{2}{\sqrt{a}}$, then there exists $\hat{d}_c$,

$$(3.1) \qquad\qquad \hat{d}_c = \frac{1}{aK + b},$$

   satisfying $\hat{d}_c \in (0, \hat{d}_M)$ such that
   - if $0 < \hat{d} < \hat{d}_c$, then $F(\lambda) > F(\mu)$;
   - if $\hat{d} = \hat{d}_c$, then $F(\lambda) = F(\mu)$;
   - if $\hat{d}_c < \hat{d} < \hat{d}_M$, then $F(\lambda) < F(\mu)$;
   - if $\hat{d} = \hat{d}_M$, then $F(\lambda) = F(\mu)$.

   Proof. If $\hat{d} \in (0, \hat{d}_M)$, two interior equilibria E_λ and E_μ exist and $\lambda < \mu$. By
(2.2), we have

$$(3.2) \qquad\qquad \lambda + \mu = \frac{1 - b\hat{d}}{a\hat{d}}, \qquad \lambda\mu = \frac{1}{a}.$$

Then

$$
\begin{aligned}
F(\lambda) - F(\mu) &= \frac{r}{mK} \left[-a(\lambda^3 - \mu^3) + (aK - b)(\lambda^2 - \mu^2) + (bK - 1)(\lambda - \mu) \right] \\
&= \frac{r(\lambda - \mu)}{mK} \left[-a((\lambda + \mu)^2 - \lambda\mu) + (aK - b)(\lambda + \mu) + (bK - 1) \right] \\
&= -\frac{r(\lambda - \mu)}{a\hat{d}^2 mK} \left[(1 - b\hat{d})^2 - a\hat{d}^2 - \hat{d}(aK - b)(1 - b\hat{d}) - a\hat{d}^2(bK - 1) \right] \\
&= -\frac{r(\lambda - \mu)}{a\hat{d}^2 mK} [1 - (aK + b)\hat{d}].
\end{aligned}
$$
(3.3)

   For $0 < K < \frac{2}{\sqrt{a}}$ and $0 < \hat{d} < \hat{d}_M$, $(aK + b)\hat{d} < (b + 2\sqrt{a})\hat{d}_M < 1$. Note that
$\lambda < \mu$; therefore, $F(\lambda) > F(\mu)$.

   For $K = \frac{2}{\sqrt{a}}$, if $\hat{d} \in (0, \hat{d}_M)$, then $(aK + b)\hat{d} < 1$, hence $F(\lambda) > F(\mu)$. It also
follows from (3.3) that $F(\lambda) = F(\mu)$ if and only if $\hat{d} = \hat{d}_M$.

   Assume that $K > \frac{2}{\sqrt{a}}$. By $F(\lambda) - F(\mu) = 0$ we obtain either $\lambda = \mu$ or

$$(3.4) \qquad\qquad 1 - (aK + b)\hat{d} = 0.$$

Hence, if $\hat{d} = \hat{d}_M$, $F(\lambda) = F(\mu)$. If $\hat{d} \in (0, \hat{d}_M)$, we can solve (3.4) to obtain $\hat{d} = \hat{d}_c$
such that the rest of the results follow. $\quad\square$

   The prey isocline $y = F(x)$ is a cubic polynomial with $\lim_{x \to -\infty} F(x) = \infty$ and
$\lim_{x \to \infty} F(x) = -\infty$. It is either decreasing or has two humps, a local minimum with
x coordinate H_m and a local maximum with x coordinate H_M, where H_m and H_M
are the solutions of the quadratic equation $F'(x) = 0$, or, equivalently,

$$(3.5) \qquad\qquad 3ax^2 - 2(aK - b)x + 1 - bK = 0.$$

Let

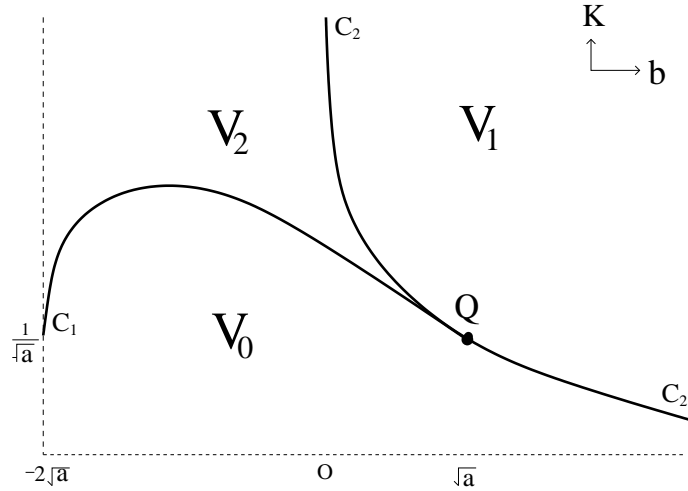$$(3.6) \qquad\qquad \Delta_1 = a^2 K^2 + abK + b^2 - 3a.$$

FIG. 3.1. *Three basic regions V_0, V_1, and V_2 in the bK plane, $Q = (\sqrt{a}, \frac{1}{\sqrt{a}})$ (See Proposition 3.2).*

Then when $\Delta_1 \geq 0$, we have

$$(3.7) \qquad H_m := \frac{1}{3a}[aK - b - \sqrt{\Delta_1}\,], \qquad H_M := \frac{1}{3a}[aK - b + \sqrt{\Delta_1}\,].$$

H_m is always to the left of H_M, i.e., $H_m \leq H_M$. The number and the position of the humps of the prey isocline inside the positive cone are determined by the signs of Δ_1 and $1 - bK$. For $K > 0$, the curve defined by $\Delta_1 = 0$ (part of an ellipse) is tangent to $1 - bK = 0$ at the point $Q(\sqrt{a}, \frac{1}{\sqrt{a}})$.

A straightforward analysis of the signs of the quantities Δ_1 and $1 - bK$ gives the following proposition.

PROPOSITION 3.2. *The two curves*

$$(3.8) \qquad \begin{aligned} &C_1 : K = \frac{1}{2a}[\sqrt{3(4a - b^2)} - b], \qquad -2\sqrt{a} \leq b \leq \sqrt{a}, \\[2mm] &C_2 : K = \frac{1}{b}, \qquad b > 0, \end{aligned}$$

divide the region $K > 0$, $b > -2\sqrt{a}$ into 3 subregions V_0, V_1, and V_2 (see Figure 3.1):

$$V_0 = \left\{ \begin{array}{c} -2\sqrt{a} < b < \sqrt{a} \\ 0 < K < \frac{1}{2a}[\sqrt{3(4a - b^2)} - b] \end{array} \right\} \cup \left\{ \begin{array}{c} \sqrt{a} \leq b \\ 0 < K < \frac{1}{b} \end{array} \right\},$$

$$V_1 = \left\{ 0 < b, \frac{1}{b} \leq K \right\},$$

$$V_2 = \left\{ \begin{array}{c} -2\sqrt{a} < b \leq 0 \\ \frac{1}{2a}[\sqrt{3(4a - b^2)} - b] < K \end{array} \right\} \cup \left\{ \begin{array}{c} 0 < b < \sqrt{a} \\ \frac{1}{2a}[\sqrt{3(4a - b^2)} - b] < K < \frac{1}{b} \end{array} \right\}.$$

(3.9)

In regions V_0, V_1, and V_2, the prey isocline has 0, 1, and 2 humps in the first quadrant, respectively (see Figure 3.2).
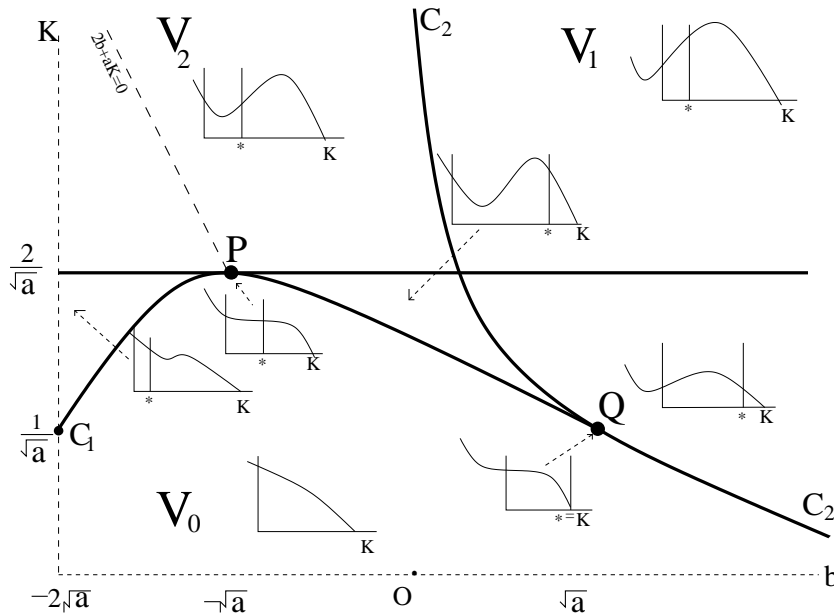
FIG. 3.2. *The positions of the two humps of the prey isocline as a function of K and b. A $*$ indicates the position of the line $x = \frac{1}{\sqrt{a}}$.*

1. Along C_1, the two humps of the prey isocline coalesce at an inflection point with x coordinate

$$H_I = \frac{aK - b}{3a} \quad (H_I = H_m = H_M).$$

2. Along C_2,
   - if $K > \frac{1}{\sqrt{a}}$, then $H_m = 0$, i.e., the left hump sits on the y-axis;
   - if $0 < K < \frac{1}{\sqrt{a}}$, then $H_M = 0$, i.e., the right hump sits on the y-axis;
   - if $K = \frac{1}{\sqrt{a}}$, then $H_m = H_M = H_I = 0$, i.e., the inflection point sits on the y-axis.

3. In region V_0, the prey isocline is decreasing and hence there are no humps inside the first quadrant.

4. In region V_1, only the right hump H_M sits inside the positive cone and
   - if $K = \frac{2}{\sqrt{a}}$, then $H_M = \frac{1}{\sqrt{a}}$,
   - if $K > \frac{2}{\sqrt{a}}$, then $H_M > \frac{1}{\sqrt{a}}$,
   - if $K < \frac{2}{\sqrt{a}}$, then $H_M < \frac{1}{\sqrt{a}}$.

5. In region V_2, both humps sit inside the first quadrant. For $(b, K) \in V_2$,
   - if $K = \frac{2}{\sqrt{a}}$ and $b < -\sqrt{a}$, then $H_m = \frac{1}{\sqrt{a}}$,
   - if $K = \frac{2}{\sqrt{a}}$ and $b > -\sqrt{a}$, then $H_M = \frac{1}{\sqrt{a}}$,
   - if $K = \frac{2}{\sqrt{a}}$ and $b = -\sqrt{a}$, i.e., at the point $P = (-\sqrt{a}, \frac{2}{\sqrt{a}})$, $H_m = H_M = \frac{1}{\sqrt{a}}$,
   - if $K > \frac{2}{\sqrt{a}}$, then $H_m < \frac{1}{\sqrt{a}} < H_M$,
   - if $K < \frac{2}{\sqrt{a}}$ and $-2\sqrt{a} < b < -\sqrt{a}$, then $\frac{1}{\sqrt{a}} < H_m < H_M$

- if $K < \frac{2}{\sqrt{a}}$ and $-\sqrt{a} < b < \sqrt{a}$, then $H_m < H_M < \frac{1}{\sqrt{a}}$.

Next we consider how the left and right humps of the prey isocline move as either b or K is varied.

PROPOSITION 3.3.

1. *For any fixed b satisfying $b > -2\sqrt{a}$, as K increases, H_M moves to the right and H_m moves to the left. Also*

$$\lim_{K \to \infty} H_M = \infty,$$

$$\lim_{K \to \infty} H_m = -\frac{b}{2a}. \quad \text{(Note that this is positive if and only if } b < 0.)$$

2. *For any fixed $K > 0$,*
   - *if $2b + aK \leq 0$ (and $-2\sqrt{a} < b < -\sqrt{a}$), as b increases,*
     - *H_M moves left,*
     - *if $0 < K < \frac{2}{\sqrt{a}}$, then H_m moves right,*
     - *if $K > \frac{2}{\sqrt{a}}$, then H_m moves left,*
     - *if $K = \frac{2}{\sqrt{a}}$, then $H_m = \frac{1}{\sqrt{a}}$;*
   3. *if $2b + aK > 0$, as b increases,*
     - *H_m moves left,*
     - *if $0 < K < \frac{2}{\sqrt{a}}$, then H_M moves right,*
     - *if $K > \frac{2}{\sqrt{a}}$, then H_M moves left,*
     - *if $K = \frac{2}{\sqrt{a}}$, then $H_M = \frac{1}{\sqrt{a}}$.*

   Also

$$\lim_{b \to -2\sqrt{a}} H_m = \frac{2 + \sqrt{a} - |\sqrt{a}K - 1|}{3\sqrt{a}},$$

$$\lim_{b \to -2\sqrt{a}} H_M = \frac{2 + \sqrt{a} + |\sqrt{a}K - 1|}{3\sqrt{a}},$$

$$\lim_{b \to \infty} H_m = -\infty,$$

$$\lim_{b \to \infty} H_M = \frac{K}{2}.$$

Proof. The limits follow from straightforward calculations.

To study the movement of the humps, we need the following derivatives from (3.7):

(3.10)
$$\frac{\partial H_M}{\partial K} = \frac{b + 2aK + 2\sqrt{\Delta_1}}{6a\sqrt{\Delta_1}},$$

$$\frac{\partial H_m}{\partial K} = \frac{-(b + 2aK) + 2\sqrt{\Delta_1}}{6a\sqrt{\Delta_1}};$$

(3.11)
$$\frac{\partial H_M}{\partial b} = \frac{2b + aK - 2\sqrt{\Delta_1}}{6a\sqrt{\Delta_1}},$$

$$\frac{\partial H_m}{\partial b} = -\frac{2b + aK + 2\sqrt{\Delta_1}}{6a\sqrt{\Delta_1}}.$$

1. Inside the region $V_1 \cup V_2$, for any fixed $b > -2\sqrt{a}$, we have $b + 2aK > 0$. By (3.10), $\frac{\partial H_M}{\partial K} > 0$, i.e., as we increase K, the right hump moves to the right. For the

left hump, by (3.10) we have

$$\frac{\partial H_m}{\partial K} = \frac{b^2 - 4a}{2a\sqrt{\Delta_1}(b + 2aK + 2\sqrt{\Delta_1})}.$$

For $b \geq 2\sqrt{a}$, the left hump does not lie inside the positive cone. Hence, if it exists, $\frac{\partial H_m}{\partial K} < 0$; i.e., as we increase K, the left hump moves left.

2. Fix K inside the region $V_1 \cup V_2$.

First note that the distance between the two humps has a minimum $\frac{2}{\sqrt{3a}}\sqrt{b^2 - a}$ along the line segment $2b + aK = 0$ when $-2\sqrt{a} \leq b \leq -\sqrt{a}$.

In the subregion where $2b + aK < 0$, by (3.11), $\frac{\partial H_M}{\partial b} < 0$, so as we increase b, the right hump moves left. The sign of

$$\frac{\partial H_m}{\partial b} = \frac{a(\frac{4}{a} - K^2)}{2\sqrt{\Delta_1}(2\sqrt{\Delta_1} - 2b - aK)}$$

indicates the direction that the left hump moves in.

Similarly, in the subregion where $2b + aK > 0$, the results follow from $\frac{\partial H_m}{\partial b} < 0$ and

$$\frac{\partial H_M}{\partial b} = \frac{a(\frac{4}{a} - K^2)}{2\sqrt{\Delta_1}(2b + aK + 2\sqrt{\Delta_1})}. \qquad \square$$

4. Hopf bifurcations. From the analysis in section 2, E_λ is the only candidate for a Hopf bifurcation. It follows from (2.7) that if a Hopf bifurcation occurs, it occurs when λ coincides with a hump of the prey isocline $y = F(x)$, i.e., when λ is such that $F'(\lambda) = 0$ or, equivalently,

$$(4.1) \qquad\qquad 3a\lambda^2 - 2(Ka - b)\lambda + 1 - Kb = 0.$$

Eliminating λ from $\hat{g}(\lambda) = 0$ and $F'(\lambda) = 0$, we obtain

$$(4.2) \quad (4a - b^2)(aK^2 + bK + 1)\hat{d}^2 + 2(abK^2 + 2(b^2 - 2a)K + b)\hat{d} + 3(1 - bK) = 0.$$

For each fixed $a > 0$, (4.2) determines the Hopf bifurcation surface $\hat{d}(b, K)$. This is illustrated in Figure 4.1. The significance of P, Q, and R will be discussed in Proposition 4.3 and Theorem 5.2.

Note that, depending on the values of a and b, there may be one or two values of $\hat{d}$ at which a Hopf bifurcation occurs. These may be found explicitly by solving (4.2) for $\hat{d}$ to obtain

$$(4.3) \qquad \hat{d}_\pm = \frac{-(abK^2 + 2(b^2 - 2a)K + b) \pm (2 + bK)\sqrt{\Delta_1}}{(4a - b^2)(aK^2 + bK + 1)}.$$

4.1. Existence of Hopf bifurcations. Our analysis is based on the positions of the humps of the prey isocline relative to the vertical line $x = \frac{1}{\sqrt{a}}$. We study the Hopf bifurcation on the surface (4.2) by fixing (b, K) in each region V_i $(i = 0, 1, 2)$ and using $\hat{d}$ as a bifurcation parameter.

THEOREM 4.1. *Fix all parameters except $\hat{d} > 0$. Provided that $H_m \neq H_M$, a generic Hopf bifurcation occurs*

1. *at $E_\lambda = (H_m, F(H_m))$, when $\hat{d} = \hat{d}_-$, if $0 < H_m < \frac{1}{\sqrt{a}}$ and*
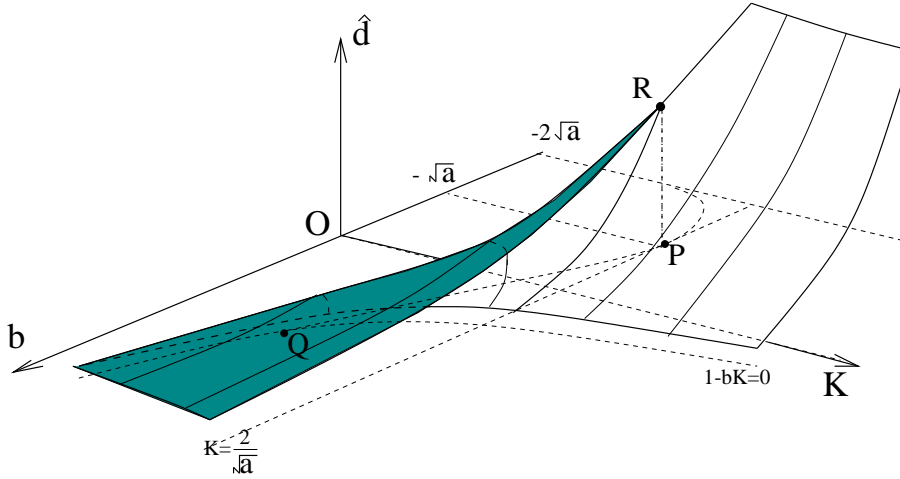
FIG. 4.1. *Hopf bifurcation surface* $\hat{d} = \hat{d}(b, K)$.

2. at $E_\lambda = (H_M, F(H_M))$, when $\hat{d} = \hat{d}_+$, if $0 < H_M < \frac{1}{\sqrt{a}}$.
No other nondegenerate Hopf bifurcations occur in the interior of the positive cone.

Proof. Consider the variational matrix about $E_\lambda = (\lambda, F(\lambda))$ (see (2.5)). It is clear from (2.2), (2.5), and (2.7) that $V(\lambda, F(\lambda))$ has pure imaginary eigenvalues if and only if $0 < \lambda < \frac{1}{\sqrt{a}}$ and $F'(\lambda) = 0$, and hence $\lambda = H_m$ or $\lambda = H_M$.

If $\lambda = H_m$, then $\hat{d} = \hat{p}(H_m)$. Substituting (3.7) in $\hat{p}(H_m)$ yields

$$\hat{d} = \hat{p}(H_m) = \frac{3[aK - b - \sqrt{\Delta_1}]}{2a^2K^2 + 2abK - b^2 + 6a - (2aK + b)\sqrt{\Delta_1}} = \hat{d}_-.$$

Similarly, if $\lambda = H_M$, then $\hat{d} = \hat{p}(H_m)$, and we can show that $\hat{p}(H_M) = \hat{d}_+$.

Next we verify the transversality condition. At E_λ with $\lambda = H_m$ or H_M, let γ be the real part of the eigenvalue. Then a straightforward calculation from (2.5) and (2.7) gives

$$(4.4) \qquad \gamma = \frac{1}{2}p(\lambda)F'(\lambda) = -\left(\frac{rm}{2K}\right)\frac{\lambda(3a\lambda^2 - 2(aK - b)\lambda + 1 - bK)}{a\lambda^2 + b\lambda + 1}.$$

Using Maple [29], we obtain

$$(4.5) \qquad \begin{aligned} \frac{\partial\gamma}{\partial\hat{d}} = -\frac{rm\frac{\partial\lambda}{\partial\hat{d}}}{27a^2K}\Big[&3a(bK - 1)(2a^2K^2 + 2abK - b^2 + 6a) \\ &- (4a^3K^3 + 3a^2bK^2 + 2b^3 - 9ab + 2)\Big(Ka - b - \sqrt{\Delta_0}\Big)\Big]. \end{aligned}$$

Note that $\frac{\partial\lambda}{\partial\hat{d}} = -\frac{\lambda}{\hat{d}\sqrt{\Delta_0}} \neq 0$ as long as $\lambda > 0$ and so $\frac{\partial\gamma}{\partial\hat{d}} = 0$ if and only if the term in square brackets in (4.5) equals 0. This occurs only when $H_m = 0$ or $H_M = 0$ or $H_m = H_M = H_I$. Thus the transversality condition is satisfied.

The only other equilibria of (1.3) are E_0, E_μ, and E_K. No nondegenerate Hopf bifurcation can occur at any of these equilibria, since the corresponding variational matrix always has real eigenvalues in each case. □
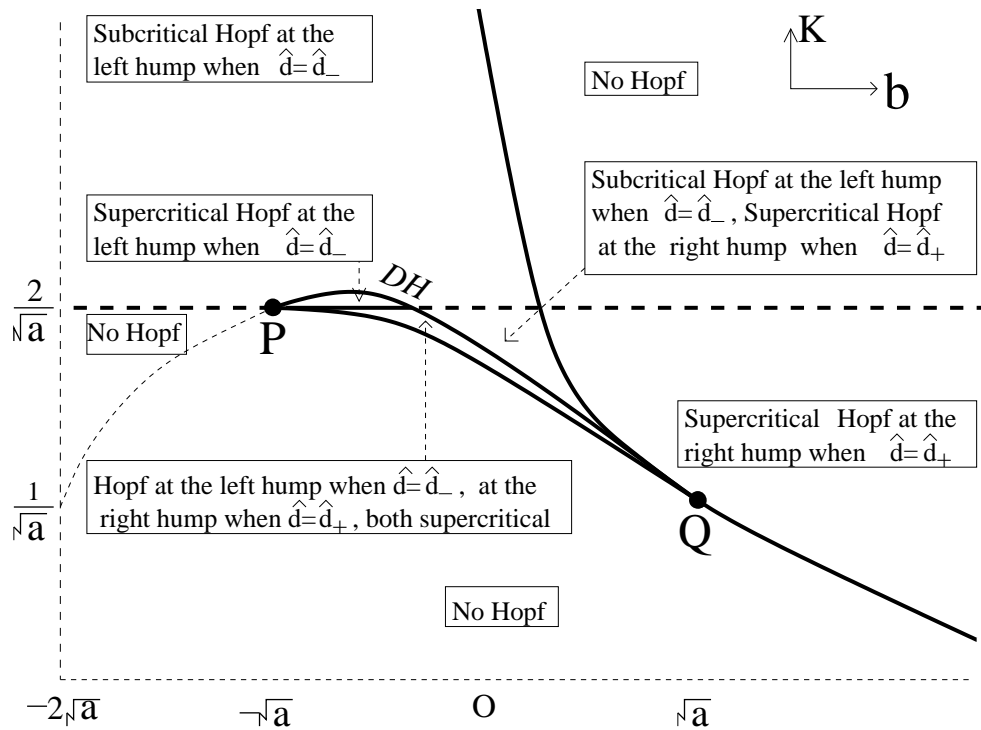
FIG. 4.2. *The existence and criticality of Hopf bifurcations in the bK plane as $\hat{d}$ is varied.*

By the above theorem, if the predator isocline has a hump inside the positive cone, and the hump is to the left of the vertical line $x = \frac{1}{\sqrt{a}}$, there exists a $\hat{d}$ defined by (4.3) such that system (1.3) undergoes a Hopf bifurcation. Hence, if we define

$$V_1^1 = \left\{ (b, K) \in V_1 \Big| K > \frac{2}{\sqrt{a}} \right\},$$

$$V_2^0 = \left\{ (b, K) \in V_2 \Big| b < -\sqrt{a}, \ K < \frac{2}{\sqrt{a}} \right\}$$

from Theorem 4.1 and Proposition 3.2 (as shown in Figure 3.2), we obtain the following corollary as illustrated in Figure 4.1 and Figure 4.2.

COROLLARY 4.2. *Fix all parameters except $\hat{d} > 0$ and allow $\hat{d}$ to vary (see Figure 4.2).*

1. *No Hopf bifurcation occurs if*
   (a) $(b, K) \in V_0 \cup V_1^1 \cup V_2^0$,
   (b) $(b, K) \in C_1$,
   (c) $(b, K) \in C_2$ *and* $K < \frac{1}{\sqrt{a}}$ *or* $K > \frac{2}{\sqrt{a}}$.
2. *There is exactly one Hopf bifurcation and it occurs at $(H_M, F(H_M))$ when $\hat{d} = \hat{d}_+$ if*
   (a) $(b, K) \in C_2$ *and* $\frac{1}{\sqrt{a}} < K < \frac{2}{\sqrt{a}}$ *or*
   (b) $(b, K) \in V_1$, $K < \frac{2}{\sqrt{a}}$.
3. *There is exactly one Hopf bifurcation and it occurs at $(H_m, F(H_m))$ when $\hat{d} = \hat{d}_-$ if*

- $(b, K) \in V_2$, $K > \frac{2}{\sqrt{a}}$.

4. *There are exactly two Hopf bifurcations: one occurs at $(H_m, F(H_m))$ when $\hat{d} = \hat{d}_-$, and the other occurs at $(H_M, F(H_M))$ when $\hat{d} = \hat{d}_+$ if*
  - $(b, K) \in V_2$, $K < \frac{2}{\sqrt{a}}$, and $b > -\sqrt{a}$.

Proof. Recall that a Hopf bifurcation occurs when $E_\lambda = (\lambda, F(\lambda))$ coincides with a hump, i.e., when either $H_m = \lambda$ or $H_M = \lambda$ with $0 < \lambda < \frac{1}{\sqrt{a}}$. The results 2(b), 3, and 4 are the consequences of Theorem 4.1 and Proposition 3.2. It remains to prove 1 and 2(a).

Now for $(b, K) \in V_0$, $y = F(x)$ has no humps. For $(b, K) \in V_1^1$, $y = F(x)$ has only one hump, with $H_M > \frac{1}{\sqrt{a}}$. For $(b, K) \in V_2^0$, $y = F(x)$ has two humps, with $\frac{1}{\sqrt{a}} < H_m < H_M$. For $(b, K) \in C_1$, $H_m = H_M = H_I$. For $(b, K) \in C_2$, if $K < \frac{1}{\sqrt{a}}, H_M = 0$; if $K > \frac{2}{\sqrt{a}}$, $H_m = 0$ and $H_M < \frac{1}{\sqrt{a}}$. Thus a Hopf bifurcation is precluded in all cases. □

4.2. Criticality of the Hopf bifurcations. In a study [30] of Hopf bifurcation in systems of the form (1.1), the following formula for the Liapunov coefficient, σ, was obtained:

$$(4.6) \qquad \sigma(x) = -\frac{p(x)F''(x)p''(x)}{p'(x)} + p(x)F'''(x) + 2p'(x)F''(x).$$

We will use this formula to give a complete description of the criticality of the Hopf bifurcation at $\hat{d} = \hat{d}_+$ and $\hat{d} = \hat{d}_-$.

PROPOSITION 4.3.
  1. *When the Hopf bifurcation occurs at E_λ with $\lambda = H_M$, it is always supercritical.*
  2. *Define the curve DH (Figures 4.1 and 4.2) connecting the two points $P(-\sqrt{a}, \frac{2}{\sqrt{a}})$ and $Q(\sqrt{a}, \frac{1}{\sqrt{a}})$:*

$$(4.7) \quad DH: \begin{array}{l} 16a^4K^4 + a^2b(8a - 3b^2)K^3 - a^2(144a - 15b^2)K^2 \\ \qquad - 8ab(9a - b^2)K + 16b^4 - 144ab^2 + 300a^2 = 0. \end{array}$$

When the Hopf bifurcation occurs at E_λ with $\lambda = H_m$, it is supercritical if $(b, K) \in V_2$ below DH; it is subcritical if $(b, K) \in V_2$ and $-2\sqrt{a} < b < -\sqrt{a}$ or above DH.
  3. *For $(b, K) \in DH$, a degenerate Hopf bifurcation occurs at E_λ with $\lambda = H_m$ when $\hat{d} = \hat{d}_-$.*

Proof. If the Hopf bifurcation occurs at E_λ with $\lambda = H_M$, it follows from (4.6) that we have

$$\begin{aligned}(4.8) \qquad \sigma(H_M) &= \frac{F''(H_M)}{p'(H_M)}[2p'^2(H_M) - p(H_M)p''(H_M)] + p(H_M)F'''(H_M) \\ &= \frac{2m^2}{(aH_M^2 + bH_M + 1)^3}\frac{F''(H_M)}{p'(H_M)} - \frac{6ra}{mK}p(H_M).\end{aligned}$$

Note that $p'(H_M) > 0$ and $F''(H_M) < 0$. It then follows from (4.8) that $\sigma < 0$, i.e., when the Hopf bifurcation occurs at $E_\lambda = (H_M, F(H_M))$ with $\hat{d} = \hat{d}_+$, it is supercritical.

Assume that when $\hat{d} = \hat{d}_-$, a Hopf bifurcation occurs at E_λ with $\lambda = H_m$. By (4.6),

$$(4.9) \qquad \sigma(\lambda) = \frac{2r[3a^2\lambda^3 - 9a\lambda - 2(b - aK)]}{K(1 - a\lambda^2)(a\lambda^2 + b\lambda + 1)}.$$

Note that when $\lambda \in (0, \frac{1}{\sqrt{a}})$, the denominator of (4.9) is positive. Consider σ defined by (4.9) as a function of b, K, and λ. Using λ as the parameter with $\lambda \in (0, \frac{1}{\sqrt{a}})$, then $\sigma = 0$ defines a simple curve connecting the two points $P(-\sqrt{a}, \frac{2}{\sqrt{a}})$ and $Q(\sqrt{a}, \frac{1}{\sqrt{a}})$. Now we develop an expression for this curve segment called DH.

If the Hopf bifurcation occurs at $x = \lambda$, then λ satisfies both (2.2) and (4.1). For the Hopf bifurcation to occur at $E_\lambda = (H_m, F(H_m))$ when $\hat{d} = \hat{d}_-$, it follows that

$$(4.10) \qquad \lambda = \frac{(2 + bK)\hat{d}_-}{3 - (b + 2aK)\hat{d}_-}.$$

Substituting (4.10) into (4.9) and using (4.3), we obtain an implicit equation $\sigma = 0$ which defines a simple curve in the bK plane, along which the Liapunov coefficient of the Hopf bifurcation vanishes. Using Maple [29], we can solve the equation and obtain $K = \frac{-b \pm \sqrt{b^2 - 4a}}{2a}$, which is not real for $-\sqrt{a} \le b \le \sqrt{a}$, and an implicit equation of b and K, which can be simplified to

$$(4.11) \qquad \begin{aligned} &16a^4 K^4 + a^2 b(8a - 3b^2)K^3 - a^2(144a - 15b^2)K^2 \\ &\quad - 8ab(9a - b^2)K + 16b^4 - 144ab^2 + 300a^2 = 0. \end{aligned}$$

For $K > 0$, (4.11) defines a cusp curve with the cusp point located at P. The upper branch of the cusp curve is above the line $K = \frac{2}{\sqrt{a}}$ and is not relevant because it is an artifact of simplification. The lower branch passes through the point Q where it is tangent to C_2. Only the curve segment DH is relevant since there are no humps for $(b, K) \in V_0$. Along the curve segment DH, the Hopf bifurcation is degenerate. One can verify that for (b, K) above the curve DH, $\sigma > 0$, and so a subcritical Hopf bifurcation occurs at the left hump. Below the curve segment DH, $\sigma < 0$, and so a supercritical Hopf bifurcation occurs at the left hump.

At the two points $P(-\sqrt{a}, \frac{2}{\sqrt{a}})$ and $Q(\sqrt{a}, \frac{1}{\sqrt{a}})$, if the Hopf bifurcation occurs, it occurs at $\lambda = \frac{1}{\sqrt{a}}$, and the associated $\sigma = 0$. The Hopf bifurcation is therefore degenerate. □

The next theorem follows from Theorem 4.1, Corollary 4.2, and Propositions 4.3.

THEOREM 4.4. *Fix all parameters except $\hat{d} > 0$ and allow $\hat{d}$ to vary (see Figures 3.2, 4.1, and 4.2).*

1. *In region $V_1 \setminus V_1^1$, a supercritical Hopf bifurcation occurs at $(H_M, F(H_M))$ when $\hat{d} = \hat{d}_+$.*
2. *In region V_2, for $K > \frac{2}{\sqrt{a}}$, above the curve DH, a subcritical Hopf bifurcation occurs at $(H_m, F(H_m))$ when $\hat{d} = \hat{d}_-$.*
3. *In region V_2, for $K > \frac{2}{\sqrt{a}}$, below the curve DH, a supercritical Hopf bifurcation occurs at $(H_m, F(H_m))$ when $\hat{d} = \hat{d}_-$.*
4. *In region V_2, for $b > -\sqrt{a}$, $K < \frac{2}{\sqrt{a}}$, below the curve DH, two Hopf bifurcations occur. When $\hat{d} = \hat{d}_-$, one occurs at $(H_m, F(H_m))$. When $\hat{d} = \hat{d}_+$, one occurs at $(H_M, F(H_M))$. They are both supercritical.*
5. *In region V_2, for $K < \frac{2}{\sqrt{a}}$, above the curve DH, two Hopf bifurcations occur. When $\hat{d} = \hat{d}_-$, one occurs at $(H_m, F(H_m))$ and is subcritical. When $\hat{d} = \hat{d}_+$, one occurs at $(H_M, F(H_M))$ and is supercritical.*
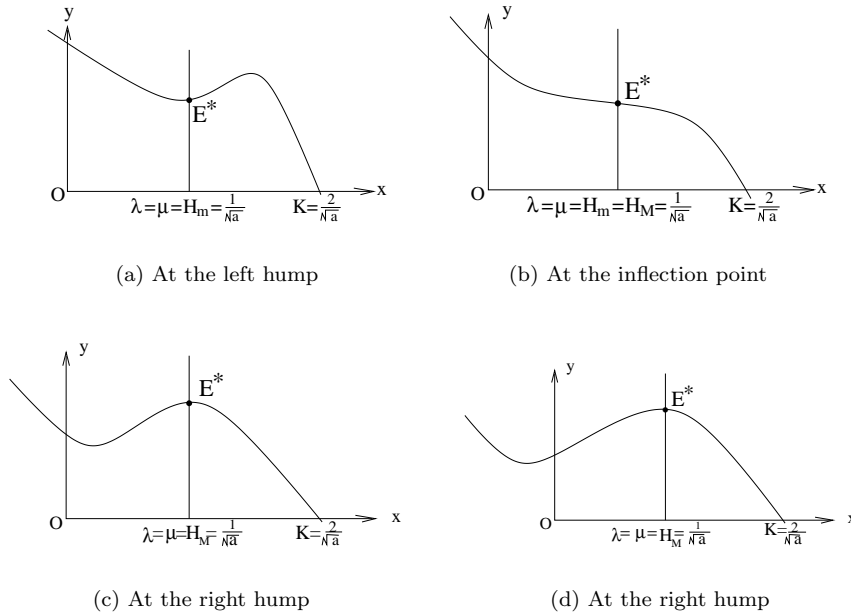
(a) At the left hump

(b) At the inflection point

(c) At the right hump

(d) At the right hump

FIG. 5.1. *Positions of the isoclines and equilibria at the cusp bifurcation of codimension* 2, (a), (c), (d), *and* 3, (b).

5. The cusp points of codimension 2 and 3.

5. The cusp points of codimension 2 and 3. From the analysis in sections 3 and 4, when

$$(5.1) \qquad K = \frac{2}{\sqrt{a}}, \qquad d = \frac{mc}{b + 2\sqrt{a}} = mc\hat{d}_M,$$

two equilibria E_λ and E_μ coalesce on the vertical line $x = \frac{1}{\sqrt{a}}$. That is,

$$E_\lambda = E_\mu = \left(\frac{1}{\sqrt{a}}, \frac{r(b + 2\sqrt{a})}{2m\sqrt{a}} \right) := E^*.$$

Using (2.6) in (2.5) it follows that the equilibrium E^* has two zero eigenvalues.

From Proposition 3.3 and Figure 5.1, the position of E^* is described below. If $b \in (-2\sqrt{a}, -\sqrt{a})$, then E^* is at the left hump (Figure 5.1(a)). As b increases in this range, the right hump moves to the left until $b = -\sqrt{a}$, when the two humps coalesce and E^* is at the inflection point (Figure 5.1(b)). For $b \in (-\sqrt{a}, \infty)$, E^* is at the right hump (Figure 5.1(c)). As b increases, the left hump moves to the left until $b = \frac{\sqrt{a}}{2}$, when the left hump reaches the y-axis and leaves the first quadrant (Figure 5.1(d)).

In this section, we prove that E^* is a cusp singularity of codimension 2 for all $b \in (-2\sqrt{a}, \infty)$ except at $b = -\sqrt{a}$ where it is a cusp singularity of codimension 3. This generalizes the results in [28] and [26]. In [28] they only consider $b = 0$, and hence the cusp singularity of codimension 2. In [26], they proved that there is a set of parameters for which there is a cusp of codimension 2 for (1.6). They also indicated that there is a cusp of codimension at least 3, but did not prove that the codimension is exactly 3.

For any $b \in (-2\sqrt{a}, \infty)$ and K, d satisfying condition (5.1), system (1.3) becomes

(5.2)
$$\begin{cases} \dot{x} = rx\left(1 - \dfrac{\sqrt{a}}{2}x\right) - \dfrac{mxy}{ax^2 + bx + 1}, \\ \dot{y} = y\left[-\dfrac{mc}{b + 2\sqrt{a}} + \dfrac{mcx}{ax^2 + bx + 1}\right], \end{cases}$$

which has a unique equilibrium E^* in the positive cone. Using a series of transformations, we shall reduce system (5.2) to normal form.

The translation

(5.3)
$$X = x - \frac{1}{\sqrt{a}}, \qquad Y = y - \frac{r(b + 2\sqrt{a})}{2m\sqrt{a}},$$

brings E^* to the origin. Expanding the right-hand side of the resulting system in a Taylor series about the origin, we obtain

(5.4)
$$\begin{cases} \dot{X} = -\dfrac{m}{b + 2\sqrt{a}}Y - \dfrac{r\sqrt{a}(b + \sqrt{a})}{2(b + 2\sqrt{a})}X^2 + R_{10}(X, Y), \\ \dot{Y} = -\dfrac{acr}{2(b + 2\sqrt{a})}X^2 + R_{20}(X, Y), \end{cases}$$

where R_{i0} $(i = 1, 2)$ is C^∞ in (X, Y) and $R_{i0}(X, Y) = O(|(X, Y)|^3)$.

Reversing time and making the transformation

$$X = X, \qquad Z = \frac{m}{b + 2\sqrt{a}}Y,$$

system (5.4) becomes

(5.5)
$$\begin{cases} \dot{X} = Z + \dfrac{r\sqrt{a}(b + \sqrt{a})}{2(b + 2\sqrt{a})}X^2 + R_{11}(X, Z), \\ \dot{Z} = \dfrac{acmr}{2(b + 2\sqrt{a})^2}X^2 + R_{21}(X, Z), \end{cases}$$

where R_{i1} $(i = 1, 2)$ is C^∞ in (X, Z) and $R_{i1}(X, Z) = O(|(X, Z)|^3)$.

Making the near-identity transformation

(5.6)
$$u = X, \qquad v = Z + \frac{r\sqrt{a}(b + \sqrt{a})}{2(b + 2\sqrt{a})}X^2 + R_{11}(X, Z),$$

we obtain

(5.7)
$$\begin{cases} \dot{u} = v, \\ \dot{v} = \delta_1 u^2 + \delta_2 uv + R_{22}(u, v), \end{cases}$$

where R_{22} is C^∞ in (X, Z), $R_{22}(u, v) = O(|(u, v)|^3)$, and

(5.8)
$$\delta_1 = \frac{acmr}{2(b + 2\sqrt{a})^2}, \qquad \delta_2 = \frac{r\sqrt{a}(b + \sqrt{a})}{(b + 2\sqrt{a})}.$$

Thus we have the following theorem.

THEOREM 5.1. *For any $b > -2\sqrt{a}$, if d and K satisfy (5.1) and $b \neq -\sqrt{a}$, then the equilibrium E^* is a cusp point of codimension 2 (a Bogdanov–Takens bifurcation point).*

If $b = -\sqrt{a}$, the cusp point is at the inflection point of $F(x)$ (Figure 5.1(b)), and by (5.8), $\delta_2 = 0$ in the normal form (5.7). Thus the Bogdanov–Takens bifurcation is degenerate and the codimension of the cusp singularity is at least 3. To show that the codimension is exactly 3, one needs to show that system (5.7) is C^∞ equivalent to the generic normal form of the cusp point of codimension 3. This is the approach taken in the following theorem.

THEOREM 5.2. *If $(b, \hat{d}, K)$ is at the point R (Figure 4.1), i.e.,*

$$(5.9) \qquad b = -\sqrt{a}, \qquad K = \frac{2}{\sqrt{a}}, \qquad d = \frac{mc}{\sqrt{a}},$$

then the equilibrium $E^* = (\frac{1}{\sqrt{a}}, \frac{r}{2m})$ is a cusp point of codimension 3 (a degenerate Bogdanov–Takens bifurcation point).

Proof. It has been shown [8, 18, 21] that any system which has a cusp point of codimension 3 is C^∞ equivalent to the following:

$$(5.10) \qquad \begin{cases} \dot{x} = y, \\ \dot{y} = x^2 + y[\beta x^3 + O(x^4)] + y^2 Q_4(x, y), \end{cases}$$

where $\beta \neq 0$. Thus, we will prove this theorem by showing that there exist smooth coordinate changes which take system (1.3) with the parameter values (5.9) into (5.10).

Under condition (5.9), $E^* = (\frac{1}{\sqrt{a}}, \frac{r}{2m})$. As in the case $b \neq -\sqrt{a}$, after translating the equilibrium to the origin and performing a Taylor expansion, we obtain

$$(5.11) \qquad \begin{cases} \dot{X} = -\dfrac{m}{\sqrt{a}} Y + \sqrt{a} m X^2 Y - \dfrac{1}{2} ar X^3 + Q_{10}(X, Y), \\[2mm] \dot{Y} = -\dfrac{1}{2} \sqrt{a} cr X^2 - mc\sqrt{a} X^2 Y + \dfrac{1}{2} arc X^3 + Q_{20}(X, Y), \end{cases}$$

where Q_{i0} $(i = 1, 2)$ is C^∞ in (X, Y) and $Q_{i0}(X, Y) = O(|(X, Y)|^4)$.

Reversing time and rescaling

$$X = X, \qquad Z = \frac{m}{\sqrt{a}} Y,$$

system (5.11) becomes

$$(5.12) \qquad \begin{cases} \dot{X} = Z - a X^2 Z + \dfrac{1}{2} ar X^3 + Q_{11}(X, Z), \\[2mm] \dot{Z} = \dfrac{crm}{2} X^2 + mc\sqrt{a} X^2 Z - \dfrac{crm\sqrt{a}}{2} X^3 + Q_{21}(X, Z), \end{cases}$$

where Q_{i1} $(i = 1, 2)$ is C^∞ in (X, Z) and $Q_{i1}(X, Z) = O(|(X, Z)|^4)$.

Using the near-identity transformation

$$(5.13) \qquad u = X, \qquad v = Z - a X^2 Z + \frac{1}{2} ar X^3 + Q_{11}(X, Z),$$

and changing u, v into x, y, we obtain

$$(5.14) \qquad \begin{cases} \dot{x} = y, \\ \dot{y} = g_1(x) + y g_2(x) + y^2 Q_2(x, y), \end{cases}$$

where

$$g_1(x) = \frac{cmr}{2}x^2 + O(x^3),$$

$$g_2(x) = \left(mc\sqrt{a} + \frac{3}{2}ra\right)x^2 - mcax^3 + O(x^4),$$

$Q_2(x,y)$ $(i = 1,2)$ is C^∞ in (x,y) and $Q_2(x,y) = O(|(X,Z)|^4)$.

Let

(5.15) $$\omega_0 = ydy - [g_1(x) + yg_2(x) + y^2 Q_2(x,y)]dx.$$

By using the 1-form (5.15) for system (5.14), we develop the normal form for the cusp singularity.

(1) Reduction of $g_1(x)$ to x^2. Since $g_1''(0) = crm \neq 0$, there exists a local diffeomorphism in x near the origin,

$$X = L(x) = \sqrt[3]{\frac{crm}{2}}x + O(x^2),$$

such that

(5.16) $$X^2 dX = g_1(x)dx.$$

By this diffeomorphism, the term $g_1(x)$ is reduced to x^2. Writing x instead of X, ω_0 becomes

(5.17) $$\omega_0 = ydy - [x^2 + yg_3(x) + y^2 Q_3(x,y)]dx,$$

where

$$g_3(x) = \alpha x^2 + \beta x^3 + O(x^4)$$

with $\alpha = (mc\sqrt{a} + \frac{3}{2}ar)\frac{\sqrt[3]{4acmr}}{acmr}$ and $\beta = -\frac{2}{r}$.

(2) Elimination of x^2 term from $g_3(x)$. Let $S(x,y) = \frac{1}{2}y^2 - \frac{1}{3}x^3$. Then $dS(x,y) = ydy - x^2 dx$. Thus

(5.18) $$yx^2 dx = y^2 dy - ydS.$$

Substituting (5.18) into (5.17), we obtain

(5.19) $$\omega_0 = (1 + \alpha y)dS(x,y) - \alpha y^2 dy - y[\beta x^3 + O(x^4) + yQ_3(x,y)]dx.$$

It follows that

(5.20)
$$\frac{\omega_0}{1 + \alpha y} = dS(x,y) - \frac{\alpha y^2}{1 + \alpha y}dy - \frac{y[\beta x^3 + O(x^4)] + yQ_4(x,y)}{1 + \alpha y}dx$$

$$= dS(x,y) - \frac{\alpha y^2}{1 + \alpha y}dy - y[\beta x^3 + O(x^4) + yQ_4(x,y)]dx,$$

where for $i = 3,4$, $Q_i(x,y)$ is C^∞ in (x,y) and $Q_i(x,y) = O(|(x,y)|^4)$. Now a near-identity transformation

(5.21) $$X = x, \quad Y = y + \cdots$$

transforms the exact 1-form $dS(x,y) - \frac{\alpha y^2}{1+\alpha y} dy$ into $dS(X,Y)$, where the term $YX^3 dX$ remains unchanged. Writing x and y instead of X and Y, system (1.3) in a neighborhood of E^* is thus equivalent to (5.10). Since $\beta = -\frac{2}{r} \neq 0$, E^* is a cusp point of codimension 3. $\quad\square$

By Theorem 5.1, if $K = \frac{2}{\sqrt{a}}$ and $d = \frac{mc}{b+2\sqrt{a}}$ but $b \neq -\sqrt{a}$, the cusp point is of codimension 2. One can find standard analysis for this codimension 2 bifurcation in Dumortier [6], Dumortier and Roussarie [7], Kuznetsov [18], and Marděsić [21]. In [28], the authors study this cusp point in the case $b = 0$ and develop a versal unfolding using K and d as distinguished parameters. The analysis of the cusp point of codimension 2 in the case $b \neq 0$ is similar; thus we will present only the codimension 3 versal unfolding of the cusp singularity. By the analysis in section 3, we have several different choices for the parameters to unfold the codimension 3 singularity: (b, d, K), (b, m, K), (b, c, K), (a, b, d), ... In this paper, we take (b, d, K) as the bifurcation parameters and develop a versal unfolding for the codimension 3 cusp singularity when these three parameters are perturbed near the point $(b_0, d_0, K_0) = (-\sqrt{a}, \frac{mc}{\sqrt{a}}, \frac{2}{\sqrt{a}})$. We study the bifurcations of this unfolding by using the results in [8] and [21].

We wish to study system (1.3) for parameters (b, d, K) in a neighborhood of $(-\sqrt{a}, \frac{mc}{\sqrt{a}}, \frac{2}{\sqrt{a}})$. Thus we let

(5.22)
$$\begin{cases} b = -\sqrt{a} + \varepsilon_1, \\ d = \frac{mc}{\sqrt{a}} + \varepsilon_2, \\ K = \frac{2}{\sqrt{a}} + \varepsilon_3 \end{cases}$$

in (1.3) and we study the bifurcations of the resulting system

(5.23)
$$\begin{cases} \dot{x} = rx\left[1 - \dfrac{x}{\frac{2}{\sqrt{a}} + \varepsilon_3}\right] - \dfrac{mxy}{ax^2 + (-\sqrt{a} + \varepsilon_1)x + 1}, \\ \dot{y} = y\left[-\left(\dfrac{mc}{\sqrt{a}} + \varepsilon_2\right) + \dfrac{mcxy}{ax^2 + (-\sqrt{a} + \varepsilon_1)x + 1}\right], \end{cases}$$

for $\varepsilon = (\varepsilon_1, \varepsilon_2, \varepsilon_3)$ sufficiently small.

THEOREM 5.3. *For parameters $\varepsilon = (\varepsilon_1, \varepsilon_2, \varepsilon_3)$ sufficiently small, system (5.23) is a generic unfolding of the cusp singularity of codimension 3.*

Proof. It has been shown in [8] that a generic unfolding, with the parameters (ν_1, ν_2, ν_3), of the codimension 3 cusp singularity is C^∞ equivalent to

(5.24)
$$\begin{cases} \dot{x} &= y, \\ \dot{y} &= \nu_1 + x^2 + y[\nu_2 + \nu_3 x + x^3 + O(x^4)] + y^2 Q(x, y). \end{cases}$$

Using the method and results of [8, 10], we will show that system (5.23), with parameters $(\epsilon_1, \epsilon_2, \epsilon_3)$, is also a generic unfolding of the codimension 3 singularity by showing that there exist smooth coordinate changes which take (5.23) into (5.24) with

$$\frac{D(\nu_1, \nu_2, \nu_3)}{D(\varepsilon_1, \varepsilon_2, \varepsilon_3)}\bigg|_{\varepsilon=(0,0,0)} \neq 0.$$

System (5.23) has a cusp point at $(\frac{1}{\sqrt{a}}, \frac{r}{2m})$ if $\varepsilon = (0,0,0)$. Applying the translation

$$\bar{x} = x - \frac{1}{\sqrt{a}}, \qquad \bar{y} = y - \frac{r}{2m},$$

and expanding system (5.23) in the power series about the origin, we have

$$(5.25) \qquad \begin{cases} \dot{\bar{x}} = \overline{L}_{11}(\bar{x}) + \bar{y}\overline{L}_{12}(\bar{x}) + \bar{y}^2 Q_{10}(\bar{x}, \bar{y}), \\ \dot{\bar{y}} = \overline{L}_{21}(\bar{x}) + \bar{y}\overline{L}_{22}(\bar{x}) + \bar{y}^2 Q_{20}(\bar{x}, \bar{y}), \end{cases}$$

where $Q_{i0}(0,0) = 0$ $(i = 1, 2)$ and

$$\overline{L}_{11}(\bar{x}) = \frac{r(a\varepsilon_3 + 2\sqrt{a}\varepsilon_1\varepsilon_3 + 2\varepsilon_1)}{2\sqrt{a}(\sqrt{a} + \varepsilon_1)(2 + \sqrt{a}\varepsilon_3)} + \frac{\sqrt{a}r\varepsilon_3}{2 + \sqrt{a}\varepsilon_3}\bar{x}$$

$$+ \frac{\sqrt{a}r(a^{3/2}\varepsilon_3 - 4\sqrt{a}\varepsilon_1 - 2\varepsilon_1^2)}{2(\sqrt{a} + \varepsilon_1)^2(2 + \sqrt{a}\varepsilon_3)}\bar{x}^2 - \frac{a^2 r}{2(\sqrt{a} + \varepsilon_1)^2}\bar{x}^3 + O(\bar{x}^4),$$

$$\overline{L}_{12}(\bar{x}) = -\frac{m}{\sqrt{a} + \varepsilon_1} + \frac{a^{3/2}m}{(\sqrt{a} + \varepsilon_1)^2}\bar{x}^2 - \frac{a^2 m}{(\sqrt{a} + \varepsilon_1)^2}\bar{x}^3 + O(\bar{x}^4),$$

$$\overline{L}_{21}(\bar{x}) = \frac{r}{2m}\left(-\varepsilon_2 - \frac{mc\varepsilon_1}{\sqrt{a}(\sqrt{a} + \varepsilon_1)}\right) - \frac{a^{3/2}cr}{2(\sqrt{a} + \varepsilon_1)^2}\bar{x}^2 + \frac{a^2 cr}{2(\sqrt{a} + \varepsilon_1)^2}\bar{x}^3 + O(\bar{x}^4),$$

$$\overline{L}_{22}(\bar{x}) = -\varepsilon_2 - \frac{mc\varepsilon_1}{\sqrt{a}(\sqrt{a} + \varepsilon_1)} - \frac{a^{3/2}cm}{(\sqrt{a} + \varepsilon_1)^2}\bar{x}^2 + \frac{a^2 mc}{(\sqrt{a} + \varepsilon_1)^2}\bar{x}^3 + O(\bar{x}^4).$$

By the transformation

$$(5.26) \qquad \tilde{x} = \bar{x}, \qquad \tilde{y} = \overline{L}_{11}(\bar{x}) + \bar{y}\overline{L}_{12}(\bar{x}) + \bar{y}^2 Q_{10}(\bar{x}, \bar{y}),$$

system (5.25) is C^∞ equivalent to

$$(5.27) \qquad \begin{cases} \dot{\tilde{x}} = \tilde{y}, \\ \dot{\tilde{y}} = L_{21}(\tilde{x}) + \tilde{y}L_{22}(\tilde{x}) + \tilde{y}^2 Q_2(\tilde{x}, \tilde{y}), \end{cases}$$

where

$$L_{21}(\tilde{x}) = \frac{r}{2a\sqrt{a}}\left((cm\varepsilon_1 - a\varepsilon_2) + O(|\varepsilon|^2)\right) + \frac{r}{2\sqrt{a}}\left(\varepsilon_3(cm\varepsilon_1 - a\varepsilon_2) + O(|\varepsilon|^3)\right)\tilde{x}$$

$$+ \left[\frac{1}{2}mcr + O(|\varepsilon|)\right]\tilde{x}^2 - \left[\frac{1}{2}\sqrt{a}cmr + O(|\varepsilon|)\right]\tilde{x}^3 + O(\tilde{x}^4),$$

$$L_{22}(\tilde{x}) = \frac{1}{2a}\left(-2mc\varepsilon_1 + 2a\varepsilon_2 + a\sqrt{a}r\varepsilon_3 + O(|\varepsilon|^2)\right) + r\left(-\varepsilon_1 + a\varepsilon_3 + O(|\varepsilon|^2)\right)\tilde{x}$$

$$- \frac{\sqrt{a}}{2}\left(3\sqrt{a}r + 2cm + O(|\varepsilon|)\right)\tilde{x}^2 + (acm + O(|\varepsilon|))\tilde{x}^3 + O(\tilde{x}^4).$$

Note that for ε sufficiently small, $c_{20}(\varepsilon) := \frac{\partial^2 L_{21}}{\partial \tilde{x}^2}(0) = \frac{1}{2}mcr + O(|\varepsilon|) \neq 0$. Thus, in the proof of Theorem 5.3, we can reduce $L_{21}(\tilde{x})$ to a quadratic polynomial without linear terms. First, by rescaling $\tilde{y}$ and time t using

$$\hat{x} = \tilde{x}, \quad \hat{y} = \tilde{y}\sqrt{c_{20}(\varepsilon)}, \quad t = \frac{1}{\sqrt{c_{20}(\varepsilon)}}\tilde{t},$$

the coefficient of $\tilde{x}^2$ in $L_{21}(\tilde{x})$ becomes $1 + O(|\varepsilon|)$, and the coefficient of $\tilde{x}$ becomes

$$c_{10}(\varepsilon) = \frac{1}{\sqrt{a}mc}\left[\varepsilon_3(mc\varepsilon_1 - a\varepsilon_2) + O(|\varepsilon|^3)\right].$$

Then the translation

(5.28) $$\hat{x} = c_{10}(\varepsilon) + O(|\varepsilon|^3) + \hat{u}, \quad \hat{y} = \hat{v},$$

brings system (5.27) to

(5.29) $$\begin{cases} \dot{\hat{u}} = \hat{v}, \\ \dot{\hat{v}} = \hat{L}_{21}(\hat{u}, \varepsilon) + \hat{v}\hat{L}_{22}(\hat{u}, \varepsilon) + \hat{v}^2\hat{Q}_2(\hat{u}, \hat{v}), \end{cases}$$

where

$$\hat{L}_{21}(\hat{u}, \varepsilon) = \hat{\nu}_1(\varepsilon) + \hat{u}^2 + O(\hat{u}^3),$$
$$\hat{L}_{22}(\hat{u}, \varepsilon) = \hat{\xi}_0(\varepsilon) + \hat{\xi}_1(\varepsilon)\hat{u} + \hat{\xi}_2(\varepsilon)\hat{u}^2 - \hat{\xi}_3(\varepsilon)\hat{u}^3 + O(\hat{u}^4),$$

and

$$\hat{\nu}_1 = \frac{1}{a\sqrt{amc}}\left(mc\varepsilon_1 - a\varepsilon_2 + O(|\varepsilon|^2)\right),$$

$$\hat{\xi}_0 = \frac{1}{a\sqrt{2rmc}}\left[-2cm\varepsilon_1 + 2a\varepsilon_2 + a\sqrt{ar}\varepsilon_3 + O(|\varepsilon|^2)\right],$$

$$\hat{\xi}_1 = \sqrt{\frac{2r}{mc}}\left(-\varepsilon_1 + a\varepsilon_3 + O(|\varepsilon|^2)\right),$$

$$\hat{\xi}_2 = \sqrt{\frac{a}{2mcr}}\left(3\sqrt{ar} + 2mc + O(|\varepsilon|)\right),$$

$$\hat{\xi}_3 = 3a\sqrt{\frac{ar}{2mc}} + O(|\varepsilon|).$$

Consider the corresponding 1-form of (5.29):

(5.30) $$\hat{v}d\hat{v} - \left[\hat{L}_{21}(\hat{u}, \varepsilon) + \hat{v}\hat{L}_{22}(\hat{u}, \varepsilon) + \hat{v}^2\hat{Q}_2(\hat{u}, \hat{v})\right]d\hat{u} = 0.$$

Now we reduce $\hat{L}_{21}(\hat{u}, \varepsilon)$ to $\tilde{\nu}_1 + \hat{u}^2$. Denote

$$\hat{L}(\hat{u}, \varepsilon) = \hat{\nu}_1(\varepsilon)\hat{u} + \frac{1}{3}\hat{u}^3 + O(\hat{u}^4).$$

Using the Malgrange preparation theorem [5], we find a coordinate change of the form

(5.31) $$\hat{u} = \Phi(\tilde{u}, \varepsilon) = \phi(\varepsilon)\tilde{u} + O(\tilde{u}^2),$$

where $\phi(0) = 1$ such that

$$\hat{L}(\Phi(\tilde{u}, \varepsilon), \varepsilon) = \tilde{\nu}_1(\varepsilon)\tilde{u} + \frac{1}{3}\tilde{u}^3,$$

and $\tilde{\nu}_1(\varepsilon) = \hat{\nu}_1(\varepsilon) + O(|\varepsilon|^2)$. Performing this coordinate change to family (5.30) and writing $\hat{v} = \tilde{v}$, we obtain

(5.32) $$\tilde{v}d\tilde{v} - \left[\tilde{L}_{21}(\tilde{u}, \varepsilon) + \tilde{v}\tilde{L}_{22}(\tilde{u}, \varepsilon) + \tilde{v}^2\tilde{Q}_2(\tilde{u}, \tilde{v})\right]d\tilde{u} = 0,$$

where

$$\tilde{L}_{21}(\tilde{u}, \varepsilon) = \hat{\nu}_1(\varepsilon) + \tilde{u}^2,$$
$$\tilde{L}_{22}(\tilde{u}, \varepsilon) = \tilde{\xi}_0(\varepsilon) + \tilde{\xi}_1(\varepsilon)\tilde{u} + \tilde{\xi}_2(\varepsilon)\tilde{u}^2 - \tilde{\xi}_3(\varepsilon)\tilde{u}^3 + O(\tilde{u}^4),$$

and $\tilde{\xi}_i(\varepsilon) = \xi_i(\varepsilon) + O(|\varepsilon|^2)$ $(i = 0, 1, 2, 3)$.

Then similar to step (2) in the proof of Theorem 5.2, using $S(\tilde{u}, \tilde{v}) = \frac{1}{2}\tilde{v}^2 - \frac{1}{3}\tilde{u}^3$, and a near-identity transformation of the form

(5.33)
$$\tilde{u} = u,$$
$$\tilde{v} = v + \frac{1}{3}\xi_2(\varepsilon)v^2 + O(v^3),$$

we eliminate the term $\tilde{v}\tilde{u}^2$ in (5.32), and system (5.23) is C^∞ equivalent to

(5.34)
$$\begin{cases} \dot{u} = v, \\ \dot{v} = \tilde{\nu}_1 + u^2 + v[\tilde{\xi}_0 + \tilde{\xi}_2 u - \tilde{\xi}_3 u^3 + O(u^4)] + v^2 Q(u, v). \end{cases}$$

For ε sufficiently small, the dominant terms in $\tilde{\nu}_1$ and $\tilde{\xi}_i$ $(i = 0, 2, 3)$ remain unchanged. Hence, we keep the previous notation.

For system (5.34), $\tilde{\xi}_3(0) = 3a\sqrt{\frac{ar}{2mc}} > 0$. Thus the rescaling

$$u = \frac{1}{\tilde{\xi}_3^{\frac{2}{5}}}U, \qquad v = \frac{1}{\tilde{\xi}_3^{\frac{3}{5}}}V, \qquad \tilde{t} = \xi_3^{\frac{1}{5}}\tau$$

shows that system (5.23) is equivalent to

(5.35)
$$\begin{cases} \dot{x} = y, \\ \dot{y} = \tilde{\nu}_1 + x^2 + y[\tilde{\tilde{\xi}}_0 + \tilde{\tilde{\xi}}_1 x - x^3 + O(x^4)] + y^2 Q(x, y), \end{cases}$$

where we have replaced (U, V, τ) with (x, y, t).

To apply the results from [8], we change the sign of the term $x^3 y$ in the second equation of (5.36) to positive by the transformation

$$\left(x, \ y, \ t, \ \tilde{\nu}_1, \ \tilde{\tilde{\xi}}_0, \ \tilde{\tilde{\xi}}_1 \right) \longrightarrow \left(x, \ -y, \ -t, \ \tilde{\nu}_1, \ -\tilde{\tilde{\xi}}_0, \ -\tilde{\tilde{\xi}}_1 \right);$$

then system (5.35) becomes

(5.36)
$$\begin{cases} \dot{x} = y, \\ \dot{y} = \tilde{\nu}_1 + x^2 + y[\tilde{\tilde{\xi}}_0 + \tilde{\tilde{\xi}}_1 x + x^3 + O(x^4)] + y^2 Q(x, y). \end{cases}$$

To simplify the expressions for the parameters, we make the rescaling

(5.37)
$$\begin{cases} \nu_1 = \sqrt[5]{\dfrac{81r^2}{4a^4(mc)^{12}}}\,\tilde{\nu}_1, \\[3mm] \nu_2 = \sqrt[10]{\dfrac{9}{64a^7r^4(mc)^6}}\,\tilde{\tilde{\xi}}_0, \\[3mm] \nu_3 = \sqrt[10]{\dfrac{64r^4}{9a^3(mc)^2}}\,\tilde{\tilde{\xi}}_1. \end{cases}$$

This yields (5.24), where using Maple, we obtain

(5.38)
$$
\begin{cases}
\nu_1 = mc\sqrt{a}(mc\varepsilon_1 + a\varepsilon_2) \\
\quad + 2(mc)^2\varepsilon_1^2 + 4amc\varepsilon_1\varepsilon_2 + a^2\varepsilon_2^2 + O(|(\varepsilon_1,\varepsilon_2)|^3), \\
\nu_2 = -2mc\varepsilon_1 - 2a\varepsilon_2 + a\sqrt{ar}\varepsilon_3 \\
\quad + \dfrac{1}{4}\left[-4(mc)^2\varepsilon_1^2 - 3a^2\sqrt{a}mcr\varepsilon_3^2 - 4a^2\varepsilon_2^2 - 16amc\varepsilon_1\varepsilon_2 \right. \\
\quad \left. + 2amc(3\sqrt{ar} + mc)\varepsilon_1\varepsilon_3 + 2a^2(\sqrt{ar} + mc)\varepsilon_2\varepsilon_3\right] + O(|\varepsilon|^3), \\
\nu_3 = -\varepsilon_1 + a\varepsilon_3 + \dfrac{1}{4}\left[-2rmc\varepsilon_1^2 - 3a^2mcr\varepsilon_3^2 - 2ar\varepsilon_1\varepsilon_2 \right. \\
\quad \left. + \sqrt{a}mc(11\sqrt{ar} + 4mc)\varepsilon_1\varepsilon_3 + 4\sqrt{a}(2\sqrt{ar} + mc)\varepsilon_2\varepsilon_3\right] + O(|\varepsilon|^3),
\end{cases}
$$

and

$$
\left.\frac{D(\nu_1,\nu_2,\nu_3)}{D(\varepsilon_1,\varepsilon_2,\varepsilon_3)}\right|_{\varepsilon=(0,0,0)} = -a^3rmc \neq 0.
$$

So system (5.23) with parameters $\varepsilon = (\varepsilon_1,\varepsilon_2,\varepsilon_3)$ is a generic family unfolding the codimension 3 cusp singularity. □

By Theorem 5.3, system (5.23) is a generic family unfolding the cusp singularity of codimension 3. So by the main theorem in [8], system (5.23) has the same bifurcation set with respect to ε_3 as (5.24) has with respect to ν, at least up to a homeomorphism in the parameter space. This bifurcation set is a cone with vertex at the origin of the parameter space.

If $\nu_1 > 0$, system (5.24) obviously has no equilibria. In a neighborhood of the origin, $\nu_1 = 0$ is a saddle-node bifurcation plane. Crossing the plane in the direction of decreasing ν_1, two equilibria are created: a saddle and an antisaddle (node or focus). Correspondingly, from (5.38), there is a surface in the parameter space $(\varepsilon_1,\varepsilon_2,\varepsilon_3)$ defined by $\nu_1(\varepsilon_1,\varepsilon_2) = 0$:

(5.39)
$$
\varepsilon_2 = -\frac{mc}{a}\varepsilon_1 + \frac{mc}{a\sqrt{a}}\varepsilon_1^2 + O(\varepsilon_1^3).
$$

Along this surface, system (5.23) has a saddle-node bifurcation. Substituting (5.22) into (2.2), it follows that the exact saddle-node bifurcation surface is given by

(5.40)
$$
\Sigma_{SN}: \quad \varepsilon_2 = -\frac{mc}{\sqrt{a}}\frac{\varepsilon_1}{\sqrt{a}+\varepsilon_1},
$$

which is consistent with (5.39). To the right of the surface Σ_{SN}, system (5.23) has no equilibria, thus all the bifurcation surfaces are located to the left of Σ_{SN}. Since up to a homeomorphism in the parameter space, each bifurcation surface is a cone with vertex at the origin; they can best be visualized by drawing their trace on the sphere

$$
S = \left\{(\nu_1,\nu_2,\nu_3)\,\middle|\,\nu_1 < 0, \nu_1^2 + \nu_2^2 + \nu_3^2 = \varepsilon_0, \varepsilon_0 > 0 \quad \text{sufficiently small}\right\}
$$

to the left of the surface Σ_{SN}.

As in Figure 5.2, let $\Gamma = S \cap \Sigma_{SN}$ be the intersection of the "half" sphere S with Σ_{SN}. Then along Γ, except for the two points b_1 and b_2, there is a saddle-node bifurcation. The next result follows from the bifurcation diagram given in Figure 3 of [8].
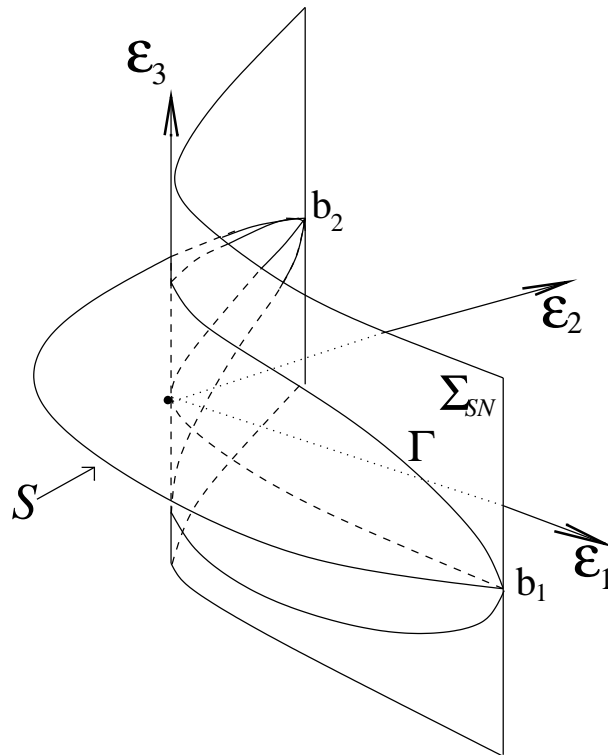
FIG. 5.2. Γ, the intersection curve of the saddle-node bifurcation surface Σ_{SN} with the half sphere S.

THEOREM 5.4. *For system* (5.24), *using* $\varepsilon = (\varepsilon_1, \varepsilon_2, \varepsilon_3)$ *as parameters, the bifur-cation diagram on S is given in Figure* 5.3.

On S, there are three bifurcation curves as shown in Figure 5.3:

- a curve H of Hopf bifurcations,
- a curve H_{om} of homoclinic bifurcations, and
- a curve SN_{lc} of saddle-node bifurcations of limit cycles.

As shown in Figure 5.3, the curve SN_{lc} joins a point h_2 on H to a point c_2 on H_{om}, and SN_{lc} is tangent to H at h_2 and tangent to H_{om} at c_2. The curves H and H_{om} have first order contact with the boundary of S at the points b_1 and b_2. In the neighborhood of b_1 and b_2, system (5.24) is an unfolding of the cusp singularity of codimension 2. This corresponds to the bifurcations along $K = \frac{2}{\sqrt{a}}$ with (d, b) in the neighborhood of $(\frac{mc}{\sqrt{a}}, -\sqrt{a})$. If $b > -\sqrt{a}$, the cusp singularity of codimension 2 is at the right hump, while if $b < -\sqrt{a}$, it is at the left hump.

Along the arc $b_1 h_2$ of the curve H, a supercritical Hopf bifurcation occurs with a stable limit cycle appearing when the arc $b_1 h_2$ is crossed from right to left. Along the arc $h_2 b_2$ of the curve H, a subcritical Hopf bifurcation occurs with an unstable limit cycle appearing when the arc $h_2 b_2$ is crossed from left to right. The point h_2 is a degenerate Hopf bifurcation point, i.e., a Hopf bifurcation point of codimension 2. The point h_2 in Figure 5.3 corresponds to the degenerate Hopf curve DH in Figures 4.2 and 6.1, which represents a three dimensional curve of codimension 2 Hopf bifurcations, projected onto the bK plane.
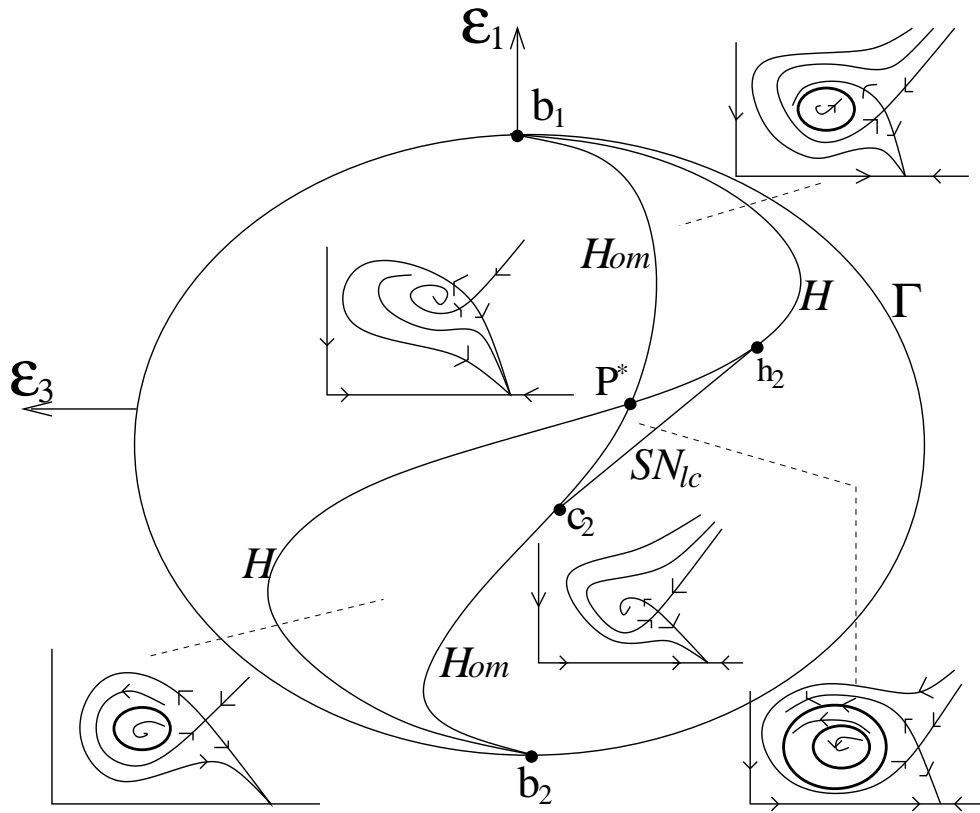
FIG. 5.3. *Bifurcation diagram for system* (5.24) *on S.*

Along the curve H_{om}, except at the point c_2, a homoclinic bifurcation of codimension 1 occurs. When the arc b_1c_2 of H_{om} is crossed from left to right, the two separatrices of the saddle point coincide and a stable limit cycle appears. The same phenomenon gives rise to an unstable limit cycle when the arc c_2b_2 of H_{om} is crossed from right to left. The point c_2 corresponds to a homoclinic bifurcation of codimension 2 (see [2, 23, 27] for references).

The curves H and H_{om} intersect transversally at a unique point P^* representing a parameter value of simultaneous Hopf and homoclinic bifurcation. The point P^* in Figure 5.3 corresponds to the curve HH in Figure 6.1, a projection to the bK plane of the three dimensional curve along which Hopf and homoclinic bifurcations occur simultaneously.

For parameter values in the curved triangle $P^*h_2c_2$, there exist exactly two limit cycles; the inner one is unstable and the outer one is stable. These two limit cycles coalesce in a generic way in a saddle-node bifurcation of limit cycles when the curve SN_{lc} is crossed from left to right. On the arc SN_{lc} itself, there exists a unique semi-stable limit cycle.

6. Global dynamics. In the previous section we proved that a degenerate Bogdanov–Takens bifurcation of codimension 3 occurs when (5.9) is satisfied. Therefore, when the parameters (1.5) are varied in a neighborhood of (5.9), a degenerate homoclinic bifurcation, degenerate Hopf bifurcation, and saddle-node bifurcation of

limit cycles must occur. In this section, using the information obtained from the analysis of the codimension 3 Bogdanov–Takens bifurcation and the geometry of system (1.3), we study the role of each of the parameters (1.5) in the global bifurcations of system (1.3). In order to do this, we determine when certain phenomena occur simultaneously. We then combine this information with the local dynamics studied in section 4 to determine the sequence of bifurcations in the different regions of parameter space as $\hat{d} = \frac{d}{mc}$ is varied.

6.1. Periodic orbits and homoclinic loops. It was proved in [30] that if system (1.3) has a limit cycle in the positive cone, it has to surround a hump of the prey isocline. In this subsection we prove several theorems which help determine whether system (1.3) has periodic orbits or homoclinic loops. Throughout this section, by periodic orbits we mean nontrivial periodic orbits.

THEOREM 6.1. *For system* (1.3), *the horizontal line* $y = F(\lambda)$ *can intersect the prey isocline* $y = F(x)$ *at most three points in the first quadrant. If there is a periodic orbit, it lies entirely to the left of* E_K *and* E_μ *(if* E_μ *exists). Furthermore,*

- *if* $\lambda \neq H_m$, H_M, *the periodic orbit must surround* E_λ *and another intersection point* $(x^*, F(x^*))$, *where* $F(x^*) = F(\lambda)$;
- *if* $\lambda = H_m$ *or* H_M, *the periodic orbit must surround* E_λ, *the tangent point of* $y = F(\lambda)$ *with* $y = F(x)$.

Proof. From (1.4) it is clear that $y = F(x)$ is a cubic polynomial and hence $y = F(\lambda)$ can intersect $y = F(x)$ at at most three points.

If $\hat{d} \geq \hat{d}_M$, then $\dot{y} \leq 0$ along all orbits and hence system (1.3) has no periodic orbits. The only case remaining is $0 < \hat{d} < \hat{d}_M$.

Using standard phase plane arguments, it is clear that any periodic orbit must lie entirely to the left of E_K and E_μ (if E_μ exists). By a consequence of the Poincaré–Bendixson theorem, a periodic orbit in the plane must surround an equilibrium. By phase plane analysis, E_λ is the only candidate.

Consider an auxiliary function of the form $L(x, y) = M(x) + N(y)$, where $M(x)$ and $N(y)$ are continuous and differentiable and satisfy the following equations, respectively:

$$p(x)M'(x) = d - cp(x), \qquad M(\lambda) = 0, \ x > 0,$$

(6.1)

$$yN'(y) = F(\lambda) - y, \qquad N(F(\lambda)) = 0, \ y > 0.$$

Solving these equations, we obtain a function $L(x, y)$ defined in the first quadrant. Along the trajectories of system (1.3) we have

(6.2) $$\frac{d}{dt}L(x, y) = (d - cp(x))[F(x) - F(\lambda)].$$

For $\hat{d} \in (0, \hat{d}_M)$, (6.2) can be rewritten as

(6.3) $$\dot{L}(t) = \frac{d}{dt}L(x(t), y(t)) = \frac{mca\hat{d}}{ax^2 + bx + 1}(x - \lambda)(x - \mu)[F(x) - F(\lambda)].$$

Denote

(6.4) $$\bar{\mu} = \min\{\mu, K\}.$$

If there is a closed orbit, $\dot{L}$ must undergo a change of sign along this orbit. If $\lambda = H_m$ or H_M, then $\dot{L}$ changes sign when $x = \lambda$, and if $\lambda \neq H_m$ or H_M, $\dot{L}$ can change

sign only when $x = \mu$ or $x = x^* \neq \lambda$, where $F(x^*) = F(\lambda)$. Therefore, $\lambda = H_m$ or H_M, and the periodic orbit surrounds E_λ, or there exists a $x^* \in (0, \lambda) \cup (\lambda, \bar{\mu})$ such that $F(x^*) = F(\lambda)$, and $(x^*, F(x^*))$ sits inside the closed orbit.   ☐

COROLLARY 6.2. *For system* (1.3), *if* E_λ *is the only intersection point of the horizontal line* $y = F(\lambda)$ *with the prey isocline* $y = F(x)$, *and* $\lambda \neq H_M$, *then there are neither periodic orbits nor homoclinic loops.*

THEOREM 6.3. *Assume* $\hat{d} \in (0, \hat{d}_M)$. *Neither periodic orbits nor homoclinic loops exist if either*

  1. $F'(x) \leq 0$ *for all* $x \in (\lambda, \bar{\mu})$, *or*
  2. $F'(\lambda) \geq 0$ *and* $F'(\mu) \geq 0$.

Proof. To prove the theorem, we make a change of variables and rescale time by setting

$$(6.5) \qquad u = \ln x, \quad v = \ln y, \quad \tau = \int_0^t \frac{1}{ax^2 + bx + 1} dt$$

to obtain

$$(6.6) \qquad \begin{cases} \dot{u} = m[F(e^u) - e^v], \\ \dot{v} = -mc\hat{g}(e^u), \end{cases}$$

where $\hat{g}(x)$ is defined in (2.2).

1. We proceed by using the Dulac criterion with the positive auxiliary function $B(v) = e^{m\beta v}$, where β is a nonnegative constant to be determined.

The divergence

$$(6.7) \qquad \begin{aligned} \mathrm{div}\,(B(v)[\dot{u}, \dot{v}]) &= -me^{m\beta v}[-e^u F'(e^u) + \beta mc\hat{g}(e^u)] \\ &= -me^{m\beta v} R(e^u, \beta), \end{aligned}$$

where

$$(6.8) \qquad \begin{aligned} R(x, \beta) &= -xF'(x) + \beta mc\hat{g}(x) \\ &= \frac{3ar}{mK} x^3 + \left(a\hat{d}mc\beta - \frac{2r(aK - b)}{mK} \right) x^2 \\ &\quad + \left[(b\hat{d} - 1)mc\beta - \frac{r(bK - 1)}{mK} \right] x + mc\beta\hat{d}. \end{aligned}$$

It follows from Theorem 6.1 that a periodic solution or a homoclinic loop must lie entirely inside the strip

$$\left\{ (x, y) \big| 0 < x < \bar{\mu}, y > 0 \right\}.$$

Thus it is enough to show that there exists a $\beta_1 \geq 0$ such that

$$(6.9) \qquad R(x, \beta_1) \geq 0, \quad x \in (0, \bar{\mu}).$$

Consider the cubic, $R(x, 0)$. By the hypothesis, $R(x, 0) > 0$ for $\lambda < x < \bar{\mu}$. Therefore (6.9) is satisfied with $\beta_1 = 0$, unless there is either one or two simple roots of $R(x, 0)$ inside the interval $(0, \lambda)$. We now consider this case.

Note that $\lim_{x \to \pm\infty} R(x, \beta) = \pm\infty$ for any $\beta \geq 0$, and $\hat{g}(\lambda) = \hat{g}(\mu) = 0$, $\hat{g}(x) < 0$ if $x \in (\lambda, \mu)$, and $\hat{g}(x) > 0$, otherwise. Therefore for $\beta > 0$, there is always one negative root of $R(x, \beta)$ and for $\beta > 0$ sufficiently small there are two positive roots in $(0, \lambda]$.

Since $R(\lambda, \beta) = -\lambda F'(\lambda) \geq 0$ for all $\beta \geq 0$, and since $\hat{g}(x) > 0$ for $x \in [0, \lambda)$, there exists $\beta_1 > 0$ such that $R(x, \beta_1)$ has a double root in $(0, \lambda]$, and thus $R(x, \beta_1) \geq 0$ for $x \in (0, \bar{\mu})$.

2. The argument is similar. Using the auxiliary function $B(v) = e^{-m\beta v}$, the divergence

$$\text{(6.10)} \qquad\qquad \text{div}\, (B(v)[\dot{u}, \dot{v}]) = me^{-m\beta v} R(e^u, \beta),$$

where $R(x, \beta) = xF'(x) + \beta mc\hat{g}(x)$. Note that $\lim_{x \to \pm\infty} R(x, \beta) = \mp\infty$ for all $\beta \geq 0$, the hypothesis implies that $F'(x) > 0$ for $\lambda < x < \mu$, and there is always a root of $R(x, \beta)$ such that $x \geq \beta$ rather than a negative root.   □

COROLLARY 6.4.

1. *Assume $K \neq \frac{2}{\sqrt{a}}$. There exists a $\tilde{d} \in (0, \hat{d}_M)$ such that for all $\hat{d} > \tilde{d}$, system (1.3) has neither periodic orbits nor homoclinic loops.*

2. *Assume $K > \frac{2}{\sqrt{a}}$. Then for all $\hat{d} > \hat{d}_c$ ($\hat{d}_c$ was defined in (3.1)), system (1.3) has neither periodic orbits nor homoclinic loops if*
   - *$(b, K) \in V_1^1$, or*
   - *$(b, K) \in V_2$ and $F(0) < F(\lambda)$.*

Proof. 1. As $\hat{d} \in (0, \hat{d}_M)$ increases, λ and μ tend to $\frac{1}{\sqrt{a}}$ monotonically from the left and right side, respectively. Hence if $K \neq \frac{2}{\sqrt{a}}$, neither the left nor the right hump is at $\frac{1}{\sqrt{a}}$, and so there exists a $\tilde{d} \in (0, \hat{d}_M)$ such that for $\hat{d} \in (\tilde{d}, \hat{d}_M)$, there are no interior equilibria or both of the interior equilibria satisfy either $F'(\lambda) > 0$ and $F'(\mu) > 0$ or $F'(x) < 0$ for all $x \in (\lambda, \bar{\mu})$. By Theorem 6.3, in either case, system (1.3) has no periodic orbits nor homoclinic loops.

2. This is a direct consequence of part 3 of Lemma 3.1 and Theorem 6.1.   □

COROLLARY 6.5. *For system (1.3) with parameters (1.5), if $(b, K) \in V_0 \cup V_2^0$, then for any $\hat{d} > 0$, system (1.3) has neither periodic orbits nor homoclinic loops.*

Proof. For any $(b, K) \in V_0$, $F'(x) < 0$ for all $x > 0$, so the result follows from Theorem 6.3.

Assume $(b, K) \in V_2^0$, and $\hat{d} \in (0, \hat{d}_M)$. In this region, $0 < \frac{1}{\sqrt{a}} < H_m < H_M < K$. By Lemma 3.1, since $K < \frac{2}{\sqrt{a}}$, $F(\lambda) > F(\mu)$. If $\mu \geq H_M$, then $F(\lambda) > F(H_M)$, and there is a unique intersection of $y = F(\lambda)$ and $y = F(x)$. The result follows from Corollary 6.2. If $\frac{1}{\sqrt{a}} < \mu < H_M$, besides $(\lambda, F(\lambda))$, any other intersection of $y = F(\lambda)$ and $y = F(x)$ must have x coordinate great than μ. The result follows from Theorem 6.1.   □

THEOREM 6.6. *Fix all parameters except $\hat{d} > 0$.*

1. *No homoclinic bifurcation can occur for $\hat{d} \in (0, \hat{d}_{\mu K})$ (where $\hat{d}_{\mu K}$ is the value of $\hat{d}$ at the transcritical bifurcation involving E_μ and E_K).*

2. *When a homoclinic bifurcation occurs,*
   - *if $F'(\mu) < 0$, then it is supercritical,*
   - *if $F'(\mu) > 0$, then it is subcritical.*

Proof. Part 1 is obvious since in this case, if E_μ does not exist, E_λ is the only equilibrium inside the positive cone and it is never a saddle. E_K cannot form a saddle loop as the x-axis is invariant. Part 2 follows from a standard result [2], since $\text{tr}(V(\mu, F(\mu))) = p(\mu)F'(\mu)$ (see (2.5)).   □

THEOREM 6.7. *Fix all parameters except $\hat{d} > 0$. For $(b, K) \in V_2$ and $K > \frac{2}{\sqrt{a}}$, there exists a $\hat{d}_l \in (\hat{d}_{\mu K}, \hat{d}_M)$ such that a homoclinic loop bifurcation involving E_μ occurs when $\hat{d} = \hat{d}_l$.*

Proof. If a homoclinic loop bifurcation occurs, it involves E_μ; hence it occurs for $\hat{d} \in (\hat{d}_{\mu K}, \hat{d}_M)$. For $\hat{d} < \hat{d}_{\mu K} (< \hat{d}_-)$, E_λ is the only equilibrium in the interior of the first quadrant and it is asymptotically stable. Since solutions are bounded, there must either be no limit cycles or an even number, excluding semistable periodic orbits. For $\hat{d} > \hat{d}_M$, system (1.3) has no limit cycles. By Corollary 4.2, there is exactly one Hopf bifurcation which occurs at $(H_m, F(H_m))$ when $\hat{d} = \hat{d}_-$ and changes the parity of the limit cycles. Therefore, there must exist a $\hat{d}_l \in (\hat{d}_{\mu K}, \hat{d}_M)$ such that a homoclinic loop bifurcation occurs to compensate for this change in the number of limit cycles.   □

6.2. Simultaneous phenomena. We will subdivide V_0, V_1, and V_2 using the curves defined below along which simultaneous phenomena occur for some $\hat{d} > 0$:

NS: a Hopf bifurcation at E_λ with $\lambda = H_m$ and a neutral saddle at E_μ
            when $\mu = H_M$;
$E_{\mu K}$:   a Hopf bifurcation at E_λ with $\lambda = H_m$ or $\lambda = H_M$ and a transcritical
            bifurcation involving E_μ and E_K;
HH: a Hopf bifurcation at E_λ with $\lambda = H_m$ and a homoclinic loop
            involving E_μ;
$Dhom$:   a homoclinic bifurcation involving E_μ when E_μ is a neutral saddle,
            i.e., $\mu = H_M$ (degenerate homoclinic bifurcation);
ST: a saddle-node bifurcation of limit cycles and a transcritical bifurcation
            involving E_μ and E_K.

In the rest of this subsection, we will find analytic expressions for curves $E_{\mu K}$ and NS and prove that curves HH and $Dhom$ must exist in certain regions in parameter space. We will prove the existence of the curve ST in the next subsection. Information about these curves is summarized in Table 6.1 and illustrated in Figure 6.1 and Figure 6.4.

PROPOSITION 6.8. *In the bK plane (Figure* 6.1*), along the curve*

$$(6.11) \qquad\qquad NS : K = -\frac{2}{b}, \qquad -\sqrt{a} < b < 0,$$

there exists a unique $\hat{d} \in (0, \hat{d}_M)$ such that a Hopf bifurcation at $(H_m, F(H_m))$ and a neutral saddle at $(H_M, F(H_M))$ occur simultaneously. To the left of NS the neutral saddle at $(H_M, F(H_M))$ occurs before the Hopf bifurcation at $(H_m, F(H_m))$. To the right of NS this ordering is reversed.

Proof. Recall from Theorem 4.1 that a Hopf bifurcation occurs at $(H_m, F(H_m))$ where $\hat{d} = \hat{d}_-$ as given in (4.3). In a similar manner to the proof of Theorem 4.1, it can be shown that for $\frac{2}{\sqrt{a}} < K < \frac{1}{b}$, a neutral saddle occurs at $(H_M, F(H_M))$ when $\hat{d} = \hat{d}_+$, as given in (4.3). We thus obtain

$$(6.12) \qquad\qquad \hat{d}_+ - \hat{d}_- = \frac{(2 + bK)\sqrt{\Delta_1}}{(4a - b^2)(aK^2 + bK + 1)}.$$

Clearly, when $K = -\frac{2}{b}$, $\hat{d}_+ = \hat{d}_- = \frac{3K}{2(aK^2 - 1)}$, thus the Hopf bifurcation and the neutral saddle occur simultaneously at this value of $\hat{d}$. Note that $b^2 - 4a < 0$. Hence when $-2\sqrt{a} < b < -\frac{2}{K}$, $\hat{d}_+ < \hat{d}_-$, the neutral saddle occurs before the Hopf bifurcation, and when $-\frac{2}{\sqrt{a}} < b < \frac{1}{K}$, the order is reversed. To complete the proof we note that $\Delta_1 = 0$ only when $\lambda = H_m = H_M = H_I = \mu$, which corresponds to the point P.   □

Recall that a transcritical bifurcation involving E_μ and E_K occurs when $K > \frac{1}{\sqrt{a}}$ and $\hat{d} = \hat{d}_{\mu K} = \hat{p}(K)$ (see (2.1)).

FIG. 6.1. *The subregions of the bK plane determined by the degenerate phenomena of Table* 6.1.

PROPOSITION 6.9. *In the bK plane (Figure* 6.1*), along the curve*

$$(6.13) \qquad E_{\mu K} : b = \frac{3 - aK^2}{K(aK^2 - 2)}, \qquad K > \sqrt{\frac{2}{a}},$$

there exists a unique $\hat{d} \in (0, \hat{d}_M)$ such that the Hopf bifurcation and the E_μ and E_K transcritical bifurcation occur simultaneously. The curve $E_{\mu K}$ is tangent to C_1 at $(0, \sqrt{3/a})$. Along this curve, if $b < 0$, the Hopf bifurcation occurs at the left hump, and if $b > 0$, the Hopf bifurcation occurs at the right hump.

1. *For $(b, K) \in V_1 \setminus V_1^1$,*
   (a) *if (b, K) is above $E_{\mu K}$, the transcritical bifurcation occurs before the Hopf bifurcation at E_λ with $\lambda = H_M$;*
   (b) *if (b, K) is below $E_{\mu K}$, the Hopf bifurcation at E_λ with $\lambda = H_M$ occurs before the transcritical bifurcation.*
2. *For $(b, K) \in V_2 \setminus V_2^0$,*
   (a) *if (b, K) is to the left of $E_{\mu K}$, the transcritical bifurcation occurs before the Hopf bifurcation at E_λ with $\lambda = H_m$;*
   (b) *if (b, K) is to the right of $E_{\mu K}$, the transcritical bifurcation occurs after the Hopf bifurcation at E_λ with $\lambda = H_m$ and, if $K < \frac{2}{\sqrt{a}}$, it occurs before the Hopf bifurcation at E_λ with $\lambda = H_M$;*
   (c) *if (b, K) is below $E_{\mu K}$, the Hopf bifurcations at E_λ with $\lambda = H_m$ and $\lambda = H_M$ occur before the transcritical bifurcation.*

Proof. Let $K = \mu$ and set $H_m = \lambda$ (see (2.4) and (3.7)),

(6.14)
$$
\begin{cases}
K = \dfrac{1 - b\hat{d} + \sqrt{\Delta_0}}{2a\hat{d}}, \\[3mm]
\dfrac{aK - b - \sqrt{\Delta_1}}{3a} = \dfrac{1 - b\hat{d} - \sqrt{\Delta_0}}{2a\hat{d}}.
\end{cases}
$$

Eliminating $\hat{d}$ from (6.14), we obtain (6.13).

Eliminating $\hat{d}$ from $\mu = K$ and $H_M = \lambda$ yields (6.13).

From Theorem 4.4 it follows that the branch of $E_{\mu K}$ with $b < 0$ corresponds to the Hopf bifurcation at $(H_m, F(H_m))$, whereas the branch with $b > 0$ corresponds to the Hopf bifurcation at $(H_M, F(H_M))$. The ordering of the Hopf bifurcation at $(H_M, F(H_M))$ and the transcritical bifurcation follows from part 1 of Proposition 3.3. As K increases across $E_{\mu K}$ with $b > 0$, the right hump moves to the right. Thus in the region above $E_{\mu K}$, the transcritical bifurcation must occur before the Hopf bifurcation at $(H_M, F(H_M))$, and in the region below, the ordering must be reversed.

To the left of $E_{\mu K}$, it follows from Proposition 6.8 that a Hopf bifurcation can occur at the same time as a neutral saddle. Thus in this region the transcritical bifurcation must occur before the Hopf bifurcation at $(H_m, F(H_m))$. To the right of $E_{\mu K}$, notice that on C_2 above Q, $H_m = 0$. When $\hat{d} = \hat{d}_{\mu K}$, $\lambda > H_m$. Fix $\hat{d}$. For K slightly below C_2, $\lambda > H_m$, but $K < \mu$. Therefore the Hopf bifurcation at $(H_m, F(H_m))$ occurs before the transcritical bifurcation in this region. $\quad\square$

For system (1.3), if $b = 0$, it was proved in [28] that the Hopf bifurcation and homoclinic bifurcation cannot occur simultaneously. However, for $b < 0$ they can happen simultaneously along the curve HH. The bifurcation analysis of the codimension 3 cusp singularity in section 5 (Theorem 5.3) indicates that in a neighborhood of the point P, there exist curves DH, HH, and $Dhom$ emanating from P:

(6.15)
$$
\begin{aligned}
DH &: K = K_{DH}(b), \\
HH &: K = K_{HH}(b), \\
Dhom &: K = K_{Dhom}(b),
\end{aligned}
$$

HH and $Dhom$ are tangent to DH at P, and $Dhom$ is to the left of HH, which is to the left of DH. Recall that an analytic expression for DH was derived (see (4.11)). For any (b, K) along HH in a neighborhood of P, there exists a $\hat{d}_l$ such that when $\hat{d} = \hat{d}_l$, the system undergoes both a Hopf bifurcation and a homoclinic loop bifurcation. For any (b, K) along $Dhom$ in a neighborhood of P, there exists a $\hat{d}_{Dhom} \in (0, \hat{d}_M)$ such that when $\hat{d} = \hat{d}_{Dhom}$, system (1.3) undergoes a degenerate (codimension 2) homoclinic loop bifurcation. Also in a neighborhood of P, for any (b, K) in the region between DH and $Dhom$, there exists a $\hat{d}_{sn} \in (0, \hat{d}_M)$ such that when $\hat{d} = \hat{d}_{sn}$, system (1.3) undergoes a saddle-node bifurcation of limit cycles. In Figure 6.1 and Figure 6.2, we use a dot-dash line to illustrate $Dhom$ and a dashed line to illustrate HH. The global extension of the curve $Dhom$ has been observed numerically using XPPAUT. In the following we prove the position of NS with respect to $Dhom$ and HH.

LEMMA 6.10. *Fix all parameters as in (1.5) except $\hat{d} > 0$. For $K < \frac{2}{\sqrt{a}}$ and $K > \frac{2}{\sqrt{a}}$ to the right of NS, if a homoclinic bifurcation occurs, it is supercritical.*

Proof. By Proposition 3.2, if $K < \frac{2}{\sqrt{a}}$, $H_M < \frac{1}{\sqrt{a}} \le \mu$. If $K > \frac{2}{\sqrt{a}}$ to the right of NS, then $H_M < \mu$. Hence in both cases, $F'(\mu) < 0$. It follows from part 2 of Theorem 6.6 that if a homoclinic bifurcation occurs in either of these cases, it is supercritical. $\quad\square$
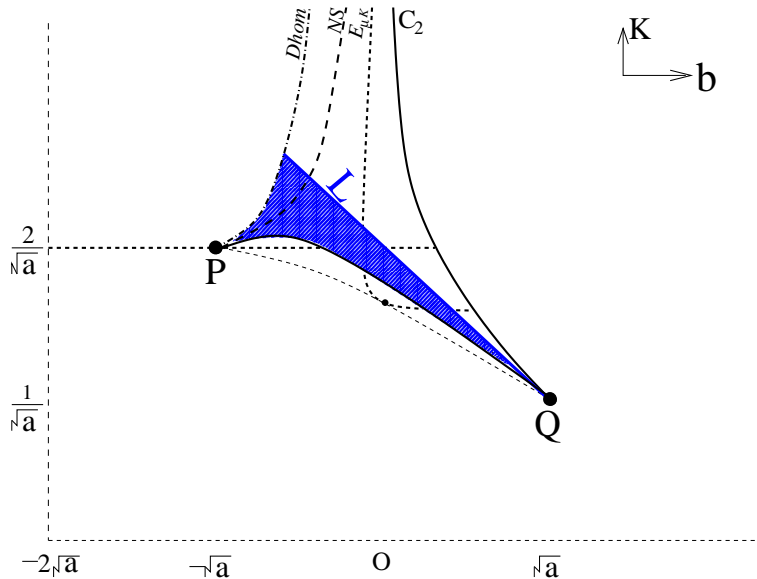
FIG. 6.2. V^*, subregion of V_2, bounded by Dhom, DH, and C_2. For $(b, K) \in V_{sn}$, the shaded region, there exists a $\hat{d}_{sn} > 0$ such that when $\hat{d} = \hat{d}_{sn}$, system (1.3) undergoes a saddle-node bifurcation of limit cycles.

COROLLARY 6.11. *Dhom lies to the left of NS.*

Before we establish the relative positions of NS and HH, we need the following results.

LEMMA 6.12.

1. *For $(b, K) \in V_2 \setminus V_2^0$ and to the left of NS, any homoclinic bifurcation that occurs must occur before the Hopf bifurcation.*

2. *For $(b, K) \in V_2$, $K \geq \frac{2}{\sqrt{a}}$ to the right of $E_{\mu K}$, any homoclinic bifurcation that occurs must occur after the Hopf bifurcation.*

3. *For $(b, K) \in V_2 \setminus V_2^0$, $K < \frac{2}{\sqrt{a}}$ to the right of $E_{\mu K}$, any homoclinic bifurcation that occurs must occur after the Hopf bifurcation at $(H_m, F(H_m))$ and before the Hopf bifurcation at $(H_M, F(H_M))$.*

4. *For $(b, K) \in V_2 \setminus V_2^0$, below $E_{\mu K}$ with $b > 0$, both Hopf bifurcations occur before any homoclinic bifurcation.*

5. *For $(b, K) \in V_1 \setminus V_1^1$, any homoclinic bifurcation that occurs must occur before the Hopf bifurcation at $(H_M, f(H_M))$ when $\hat{d} = \hat{d}_+$.*

Proof. 1. For $(b, K) \in V_2 \setminus V_2^0$ and to the left of NS, from Theorem 4.4 and Proposition 6.8, the Hopf bifurcation at $(H_m, F(H_m))$ with $\hat{d} = \hat{d}_-$ occurs after the neutral saddle at $(H_M, F(H_M))$ with $\hat{d} = \hat{d}_+$. This implies that for $\hat{d} \geq \hat{d}_+$ $H_m \leq \lambda \leq \mu < H_M$, and hence $F'(\lambda) \geq 0$ and $F'(\mu) > 0$. By part 2 of Theorem 6.3, there are no periodic orbits or homoclinic loops for $\hat{d} \geq \hat{d}_+$.

2. For $(b, K) \in V_2$ and $K \geq \frac{2}{\sqrt{a}}$, it follows from Theorem 4.4 that the only Hopf bifurcation that occurs is at the $(H_m, F(H_m))$ when $\hat{d} = \hat{d}_-$, and it is subcritical. By part 2(b) of Proposition 6.9, the Hopf bifurcation occurs before the E_μ and E_K transcritical bifurcation. Hence by part 1 of Theorem 6.6, no homoclinic bifurcation occurs for $\hat{d} \in (0, \hat{d}_-]$.

3. For $(b, K) \in V_2$ and $K < \frac{2}{\sqrt{a}}$, by part 2(b) of Proposition 6.9, the transcritical bifurcation involving E_μ and E_K occurs after the Hopf bifurcation at $(H_m, F(H_m))$ when $\hat{d} = \hat{d}_-$ and before the Hopf bifurcation at $(H_M, F(H_M))$ when $\hat{d} = \hat{d}_+$. A similar argument to that for part 2 shows that no homoclinic bifurcation occurs in $(0, \hat{d}_-]$, and a similar argument to that for part 1 shows that no homoclinic bifurcation occurs for $\hat{d} \geq \hat{d}_+$.

4. For $(b, K) \in V_2 \setminus V_2^0$, below $E_{\mu K}$ $(b > 0)$, by Theorem 4.4, Hopf bifurcations occur at E_λ when $\lambda = H_m$ and $\lambda = H_M$. But by part 2(c) of Proposition 6.9, both Hopf bifurcations occur before the transcritical bifurcation involving E_μ and E_K, which implies any homoclinic bifurcation must occur after both Hopf bifurcations.

5. For $(b, K) \in V_1 \setminus V_1^1$, by Theorem 4.4, there is one Hopf bifurcation at $(H_M, F(H_M))$ when $\hat{d} = \hat{d}_+$. If $\hat{d} \geq \hat{d}_+$, then $H_M \leq \lambda < \bar{\mu}$ and $F'(x) \leq 0$ for $x \in (\lambda, \bar{\mu})$. Thus by part 1 of Theorem 6.3, for $\hat{d} \geq \hat{d}_+$ no homoclinic loops can exist. Hence any homoclinic bifurcation that occurs must occur before the Hopf bifurcation. □

PROPOSITION 6.13. *Fix all the parameters in* (1.5) *except* $\hat{d} > 0$. *If* (b, K) *is outside the region bounded by* NS, C_1, *and* $E_{\mu K}$ *(Figure* 6.1*), for all* $\hat{d} \in (0, \hat{d}_M)$, *a Hopf bifurcation and a homoclinic bifurcation cannot occur simultaneously.*

Proof. It follows from Theorem 4.4 that no Hopf bifurcations can occur for (b, K) in the regions V_0, V_2^0, and V_1^1. The proofs for $V_1 \setminus V_1^1$ and $V_2 \setminus V_2^0$ follow from Lemma 6.12. □

Recall that in the neighborhood of P, there exists a curve HH along which the Hopf bifurcation at the left hump and a homoclinic bifurcation occur simultaneously. Let V_{HH} be the region bounded by curves NS, $K = \frac{2}{\sqrt{a}}$, and $E_{\mu K}$ $(b < 0)$. Now we prove the following theorem regarding the extension of the curve HH in V_{HH}.

THEOREM 6.14. *Fix all parameters except* $\hat{d} > 0$. *In* V_{HH}, *there exists a curve* HH: $K = K_{HH}(b)$ *with finite end point at* $P(-\sqrt{a}, \frac{2}{\sqrt{a}})$ *(Figure* 6.1*). For any* $(b, K) \in HH$, *there exists a unique* $\hat{d}_{hh} \in (\hat{d}_{\mu K}, \hat{d}_M)$, *such that when* $\hat{d} = \hat{d}_{hh}$, *the subcritical Hopf bifurcation at* $(H_m, F(H_m))$ *and a homoclinic loop bifurcation occur simultaneously.*

Proof. By Theorem 6.7, for $(b, K) \in V_{HH}$ there exists $\hat{d}_l \in (\hat{d}_{\mu K}, \hat{d}_M)$ such that a homoclinic bifurcation occurs at $\hat{d} = \hat{d}_l$. By Proposition 6.13, if the curve $K = K_{HH}(b)$ exists, it lies inside the region V_{HH}.

Now we prove that in V_{HH}, for fixed $K > \frac{2}{\sqrt{a}}$, there exists a $b \in (-\frac{2}{K}, \frac{3-aK^2}{K(aK^2-2)})$ such that the subcritical Hopf bifurcation at the left hump and a homoclinic bifurcation involving E_μ happen simultaneously when $\hat{d} = \hat{d}_-(< \hat{d}_+)$.

(a) First we show that along NS, any homoclinic bifurcation at $\hat{d} = \hat{d}_l$ occurs before the Hopf bifurcation.

From Proposition 6.8, if $b = -\frac{2}{K}$ (i.e., $(b, K) \in NS$), a Hopf bifurcation at $(H_m, F(H_m))$ and a neutral saddle at $(H_M, F(H_M))$ occur simultaneously when $\hat{d} = \frac{3K}{2(ak^2-1)}$. Then for $\hat{d} \in [\frac{3K}{2(aK^2-1)}, \hat{d}_M)$, we have $F'(\lambda) \geq 0$ and $F'(\mu) \geq 0$. By Theorem 6.3 neither periodic orbits nor homoclinic loops can exist. Hence along NS, any homoclinic bifurcation occurs before the Hopf bifurcation.

(b) Next we show that along $E_{\mu K}$, the Hopf bifurcation occurs before any homoclinic bifurcation.

This is obvious since the Hopf bifurcation occurs at $\hat{d} = \hat{d}_{\mu K}$, and any homoclinic bifurcation occurs when $\hat{d} > \hat{d}_{\mu K}$.

TABLE 6.1
Curves in the bK plane corresponding to degenerate phenomena. For the last 7 curves, there exists a $\hat{d}$ such that the indicated bifurcation occur.

Name	Phenomenon	Expression	
C_1	$H_m = H_M$	$K = \frac{\sqrt{3(4a-b^2)}-b}{2a},$ $-2\sqrt{a} < b \le \sqrt{a}$	(3.8)
C_2	$H_m = 0$ or $H_M = 0$	$K = \frac{1}{b}, \ \ b > 0$	(3.8)
$E_{\mu K}$	Hopf & $E_\mu - E_K$ transcritical	$b = \frac{3 - aK^2}{K(aK^2 - 2)}$	(6.13)
NS	Hopf & neutral saddle	$K = -\frac{2}{b}$	(6.11)
BT	Bogdanov–Takens	$K = \frac{2}{\sqrt{a}}$	(5.1)
DH	Degenerate Hopf	$\sigma(K, b) = 0$	(4.11)
HH	Hopf & homoclinic	$K = K_{HH}(b)$	Theorem 6.14
$Dhom$	Degenerate homoclinic	$K = K_{Dhom}(b)$	(6.15)

By (a) and (b), for any K with (b, K) in V_{HH} there exists at least one $b^* \in (-\frac{2}{K}, \frac{3-aK^2}{K(aK^2-2)})$ such that at (b^*, K), there exists a unique $\hat{d} \in (\hat{d}_{\mu K}, \hat{d}_M)$ such that a Hopf bifurcation and a homoclinic loop bifurcation occur simultaneously. □

Remark 6.15. Theorem 5.4 proves the local existence of the curve HH emanating from P and lying between the curves NS and DH. Theorem 6.14 shows that this curve may be globally extended into the region V_{HH}. Since both NS and $E_{\mu K}$ tend to $b = 0$ as $K \to \infty$, the global extension of HH should do the same. In Figure 6.1 we have drawn the curve HH as a single branch emanating from P and lying above DH in V_{HH}. This representation of HH is supported by numerical simulations using XPPAUT [11]; however, we have not been able analytically to preclude that HH has multiple branches or crosses the curve DH.

We summarize the relevant curves in the bK plane in Table 6.1. As shown in Figure 6.1, we use these curves to divide V_0, V_1, and V_2 into the following subregions:

$$V_0 = V_0^1 \cup V_0^2,$$

$$V_1 = \bigcup_{k=1}^{4} V_1^k,$$

$$V_2 = \bigcup_{k=0}^{11} V_2^k.$$

6.3. Saddle-node bifurcation of limit cycles. Let V^* be the subregion of V_2 (Figure 6.1) bounded by $Dhom$, DH, and C_2; i.e.,

(6.16) $$V^* = V_2^1 \cup V_2^2 \cup V_2^6 \cup V_2^8 \cup V_2^9 \cup V_2^{10}.$$

To study the saddle-node bifurcation of limit cycles for parameters away from P, we introduce a line segment L in the following proposition (see Figure 6.2).

PROPOSITION 6.16. *In the bK plane, the line*

(6.17) $$L : \quad K = -\frac{b}{a} + \frac{2}{\sqrt{a}}$$

lies between the curves C_2 and DH and is tangent to C_1, DH, and C_2 at Q. In region V_2, below this line, $F(0) > F(H_M)$; above the line, $F(0) < F(H_M)$; and on the line, $F(0) = F(H_M)$.

Proof. The proof follows from direct calculations. □

As shown in Figure 6.2, the line L subdivides the region V^* into two subregions. Denote the shaded subregion below L by

$$V_{sn} = \left\{ (b, K) \in V^* \,\middle|\, K < -\frac{b}{a} + \frac{2}{\sqrt{a}} \right\}.$$

PROPOSITION 6.17. *Fix all the parameters except $\hat{d} > 0$. If $(b, K) \in V_{sn}$, there exists a $\hat{d}_{sn} \in (0, \hat{d}_-)$ such that when $\hat{d} = \hat{d}_{sn}$, system (1.3) undergoes a saddle-node bifurcation of limit cycles.*

Proof. For $(b, K) \in V_{sn}$, it follows from Proposition 6.16 that there exists a $\hat{d}_0 > 0$ such that for $\hat{d} \in (0, \hat{d}_0)$, $F(\lambda) > F(H_M)$. By Corollary 6.2, system (1.3) has neither periodic orbits nor homoclinic loops for $(b, K) \in V_{sn}$ and $\hat{d} \in (0, \hat{d}_0)$. Further, it follows from Theorem 4.4 that there exists a $\hat{d}_- \in [\hat{d}_0, \hat{d}_M)$ such that when $\hat{d} = \hat{d}_-$, system (1.3) undergoes a subcritical Hopf bifurcation at $(H_m, F(H_m))$. Recall that E_λ is asymptotically stable for $0 < \hat{d} < \hat{d}_-$ (see Table 2.1) and so an unstable periodic orbit must be destroyed as $\hat{d}$ increases through $\hat{d}_-$.

(1) In V_{sn} for $K \geq \frac{2}{\sqrt{a}}$ and to the right of the curve NS, from Theorem 4.4, there are no other Hopf bifurcations. From Lemma 6.10 any homoclinic bifurcation that occurs in supercritical. Thus, the only way to create the unstable limit cycle that must be destroyed in the subcritical Hopf bifurcation is to first have a saddle-node bifurcation of limit cycles.

(2) In V_{sn} for $K < \frac{2}{\sqrt{a}}$, by part 5 of Theorem 4.4, in addition to the subcritical Hopf bifurcation at $\hat{d} = \hat{d}_-$, and there is a supercritical Hopf bifurcation at $\hat{d} = \hat{d}_+$. From Lemma 6.10, any homoclinic bifurcation that occurs is supercritical. By a similar argument as for case (1), there must be a saddle-node bifurcation of limit cycles before the two Hopf bifurcations.

(3) In V_{sn} for $K \geq \frac{2}{\sqrt{a}}$, by Theorem 6.7 there exists a $\hat{d}_l$ such that when $\hat{d} = \hat{d}_l$ system (1.3) undergoes a homoclinic bifurcation. By Lemma 6.12, this homoclinic bifurcation must occur before the Hopf bifurcation. By definition, to the right of $Dhom$ there must be a supercritical homoclinic bifurcation. Thus, an unstable limit cycle must already surround the asymptotically stable equilibrium. This limit cycle must have been created by a saddle-node bifurcation of limit cycles. □

PROPOSITION 6.18.

1. *In the bK plane (Figure 6.3), the curve*

(6.18) $$C_{sn} : \quad b = \frac{3 - aK^2}{K}, \quad K \geq \sqrt{\frac{3}{a}}$$

lies between the curves C_1 and $E_{\mu K}$ and is tangent to them at $(0, \sqrt{3/a})$. For $(b, K) \in V_{sn}$, below this curve, if $\hat{d} \in (0, \hat{d}_{\mu K})$, system (1.3) has no closed orbits. Therefore the saddle-node bifurcation of limit cycles must occur after the transcritical bifurcation involving E_μ and E_K.
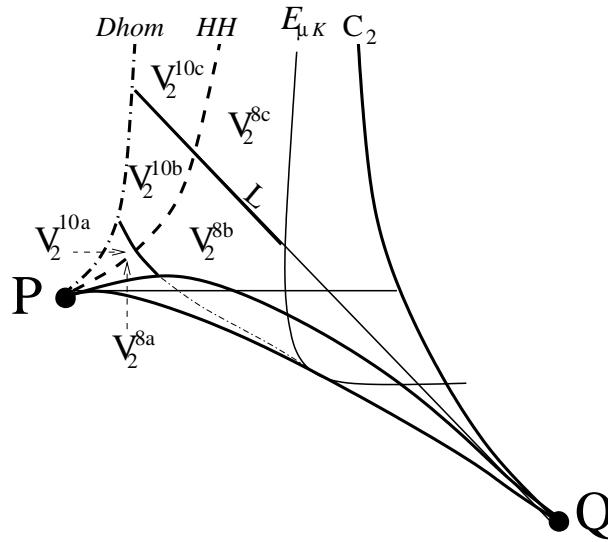
FIG. 6.3. *In the shaded subregion of V_{sn} below C_{sn}, the saddle-node bifurcation of limit cycles occurs after the transcritical bifurcation involving E_μ and E_K. In the shaded subregion of V_{sn} to the right of $E_{\mu K}$, the saddle-node bifurcation of limit cycles occurs before the transcritical bifurcation.*

2. *For $(b, K) \in V_{sn}$ to the right of the branch of $E_{\mu K}$ with $b < 0$, a saddle-node bifurcation of limit cycles occurs before the transcritical bifurcation involving E_μ and E_K.*

Proof. Note that in V_{sn}, $F(0) > F(H_M)$. As $\hat{d}$ increases from 0, there exists a $\hat{d}_0$ such that for $\hat{d} = \hat{d}_0$, $\lambda = \lambda_0$ where $F(\lambda_0) = F(H_M)$ and $\lambda_0 < H_m$. By Corollary 6.2, for $0 < \hat{d} < \hat{d}_0$, there are no periodic orbits or homoclinic loops. Therefore, the saddle-node bifurcation of limit cycles must occur for some $\hat{d} > \hat{d}_0$.

Setting $\mu = K$ and $F(\lambda) = F(H_M)$ in (1.4), (2.4), and (3.7) and eliminating $\hat{d}$, we obtain (6.13) and (6.18). By Proposition 6.9, if (b, K) satisfies (6.13), then when $\hat{d} = \hat{d}_{\mu K}$, we have $\lambda = H_m$. Hence (6.13) is not relevant and (6.18) corresponds to $\hat{d}_{\mu K} = \hat{d}_0$. Straightforward calculations show that curve (6.18) lies between C_1 and $E_{\mu K}$, is tangent to both C_1 and $E_{\mu K}$ at $(0, \sqrt{3/a})$, and lies below L in V_{sn}. Consideration of the sign of $F(\lambda) - F(H_M)$ when $\hat{d} = \hat{d}_{\mu K}$ shows that for $(b, K) \in V_{sn}$ below curve (6.18), $\hat{d}_0 > \hat{d}_{\mu K}$, and above curve (6.18), $\hat{d}_0 < \hat{d}_{\mu K}$. Therefore, the result follows.

On the other hand, for $(b, K) \in V_{sn}$ to the right of the branch of the curve $E_{\mu K}$ with $b < 0$, the Hopf bifurcation at $(H_m, F(H_m))$ occurs at the same time as or before the transcritical bifurcation involving E_μ and E_K. By Proposition 6.17, for $(b, K) \in V_{sn}$, the Hopf bifurcation at $(H_m, F(H_m))$ occurs after the saddle-node bifurcation of limit cycles. Therefore in this region a saddle-node bifurcation of limit cycles must occur before the transcritical bifurcation.   □

As shown in Figure 6.4, the segment of C_{sn} between *Dhom* and *DH* and the segment of L between *Dhom* and $E_{\mu K}$ divide the regions V_2^8 and V_2^{10} into subregions V_2^{ia}, V_2^{ib}, and V_2^{ic} ($i = 8, 10$). For the saddle-node bifurcation of limit cycles and its

FIG. 6.4. In V_{sn}, the curve C_{sn} and line L divide the regions V_2^8 and V_2^{10} into subregions V_2^{ia}, V_2^{ib}, and V_2^{ic} $(i = 8, 10)$.

relative order with respect to the transcritical bifurcation involving E_μ and E_K, we make the following remark.

Remark 6.19.

1. By Proposition 6.18, for (b, K) in V_2^{8a} and V_2^{10a}, the saddle-node bifurcation of limit cycles occurs after the transcritical bifurcation involving E_μ and E_K.

2. When $\hat{d} = 0$, system (1.3) has a degenerate graphic with a line segment of equilibria. The bifurcation analysis of this type of graphic is very complicated (see [9] for reference), and will appear elsewhere.

3. For (b, K) in V_2^{ic} $(i = 8, 10)$ and V_2^9, above the line L, a saddle-node bifurcation of limit cycles may occur or the required limit cycles may come from a bifurcation of the degenerate singularity when $\hat{d} = 0$. Numerical simulations show that for (b, K) in V_2^{ic} $(i = 8, 10)$ and V_2^9, above the line L, system (1.3) has two limit cycles for $\hat{d} > 0$ very small.

4. For (b, K) in V_2^{ib} $(i = 8, 10)$ and V_2^6, it follows from Proposition 6.18 that there exists a curve that lies between C_{sn} and $E_{\mu K}$. For (b, K) on this curve, there exists a $\hat{d}_{sn} > 0$ such that a saddle-node bifurcation of limit cycles and the transcritical bifurcation involving E_μ and E_K occur simultaneously. This curve ST may not be unique.

6.4. Sequences of bifurcations. Although a three dimensional Hopf bifurcation surface is shown in Figure 4.1, it is not convenient to visualize the entire bifurcation diagram for system (1.3) in $(b, \hat{d}, K)$ space. Instead we describe the bifurcation diagram as $\hat{d}$ varies for fixed b and K inside each subregion (see Figure 6.1) of the bK plane. The sequences of bifurcations that occur in the interior of each subregion are given using the "dictionary of phase portraits" in Table 6.2. The sequences on the boundaries of each subregion are not included. These can easily be deduced by reading Tables 6.3–6.5 vertically. On the boundaries various simultaneous or degenerate bifurcations occur.
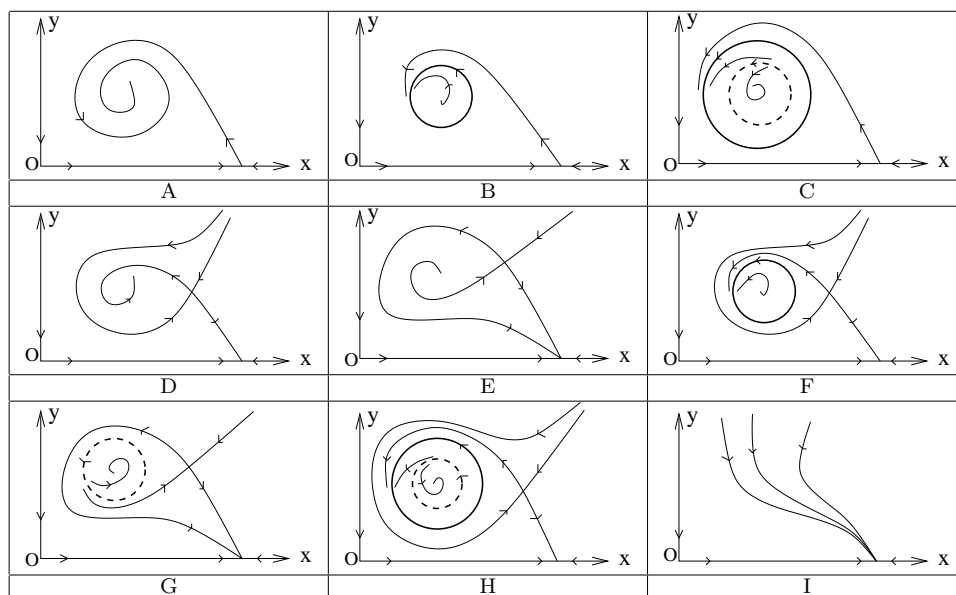
TABLE 6.2
Dictionary of phase portraits.

TABLE 6.3
Sequences of phase portraits for $(b, K) \in V_0$.

V_0^1	A	D	I
	$(0, \hat{d}_{\mu K})$	$(\hat{d}_{\mu K}, \hat{d}_M)$	$(\hat{d}_M, \infty)$

V_0^2	A	I	
	$(0, \hat{d}_{\lambda K})$	$(\hat{d}_{\lambda K}, \infty)$	

THEOREM 6.20. *Fix all parameters except $\hat{d} > 0$. For $(b, K) \in V_0$, when $\hat{d} > 0$ increases, the sequence of phase portraits occurring in the interior of each subregion is given in Table 6.3. In the table, moving from left to right as $\hat{d}$ increases, the phase portrait changes as a result of one of the following bifurcations:*

- *the transcritical bifurcation involving E_λ and E_K that occurs at $\hat{d} = \hat{d}_{\lambda K}$;*
- *the transcritical bifurcation involving E_μ and E_K that occurs at $\hat{d} = \hat{d}_{\mu K}$;*
- *the saddle-node bifurcation involving E_λ and E_μ that occurs at $\hat{d} = \hat{d}_M$.*

Proof. By Corollary 6.5, system (1.3) has neither periodic orbits nor homoclinic loops for $(b, K) \in V_0$. As $\hat{d} \in (0, \hat{d}_M)$ is varied, if $K > \frac{1}{\sqrt{a}}$, the only bifurcation that can occur is the transcritical bifurcation involving E_μ and E_K that occurs when $\hat{d} = \hat{d}_{\mu K}$ and the saddle-node bifurcation that occurs when $\hat{d} = \hat{d}_M$. If $0 < K < \frac{1}{\sqrt{a}}$, the only bifurcation that can occur is the transcritical bifurcation involving E_λ and E_K that occurs when $\hat{d} = \hat{d}_{\lambda K}$. $\quad\square$

THEOREM 6.21. *Fix all parameters except $\hat{d} > 0$. For $(b, K) \in V_1$, when $\hat{d} > 0$ increases, the sequence of phase portraits occurring in the interior of each subregion is given in Table 6.4. In the table, moving from left to right as $\hat{d}$ increases, the phase*

TABLE 6.4
Sequences of phase portraits for $(b, K) \in V_1$.

V_1^1	B	F	E	I
	$(0, \hat{d}_{\mu K})$	$(\hat{d}_{\mu K}, \hat{d}_l)$	$(\hat{d}_l, \hat{d}_M)$	$(\hat{d}_M, \infty)$
V_1^2	B	F	D	I
	$(0, \hat{d}_{\mu K})$	$(\hat{d}_{\mu K}, \hat{d}_+)$	$(\hat{d}_+, \hat{d}_M)$	$(\hat{d}_M, \infty)$
V_1^3	B	A	D	I
	$(0, \hat{d}_+)$	$(\hat{d}_+, \hat{d}_{\mu K})$	$(\hat{d}_{\mu K}, \hat{d}_M)$	$(\hat{d}_M, \infty)$
V_1^4	B	A	I	
	$(0, \hat{d}_+)$	$(\hat{d}_+, \hat{d}_{\lambda K})$	$(\hat{d}_{\lambda K}, \infty)$	

portrait changes due to one of the following bifurcations:

- *the transcritical bifurcation involving E_λ and E_K that occurs at $\hat{d} = \hat{d}_{\lambda K}$;*
- *the transcritical bifurcation involving E_μ and E_K that occurs at $\hat{d} = \hat{d}_{\mu K}$;*
- *the saddle-node bifurcation involving E_λ and E_μ that occurs at $\hat{d} = \hat{d}_M$;*
- *the supercritical Hopf bifurcation that occurs when $\hat{d} = \hat{d}_+$;*
- *a supercritical homoclinic bifurcation that occurs when $\hat{d} = \hat{d}_l$.*

For $(b, K) \in V_1^3 \cup V_1^4$, the sequence is complete up to an even number of saddle-node bifurcations of limit cycles. For $(b, K) \in V_1^1 \cup V_1^2$, the sequences are complete up to an even number of saddle-node bifurcations of limit cycles and an even number of extra supercritical homoclinic bifurcations.

Proof. In V_1 for $\hat{d} > 0$ sufficiently small, E_λ is an unstable node. Since solutions are bounded, a simple phase plane argument shows that there must be a stable limit cycle surrounding E_λ.

If $(b, K) \in V_1^1$, by Theorem 4.4, system (1.3) does not undergo Hopf bifurcations. Thus there must exist $\hat{d}_l$ such that when $\hat{d} = \hat{d}_l$ there is a supercritical homoclinic bifurcation destroying the limit cycle described above. Further, a transcritical bifurcation involving E_μ and E_K occurs when $\hat{d} = \hat{d}_{\mu K}$. By Theorem 6.6, $\hat{d}_{\mu K} < \hat{d}_l$. Thus, for $\hat{d} \in (0, \hat{d}_{\mu K})$, the system has a stable periodic orbit. For $\hat{d} \in (\hat{d}_l, \hat{d}_M)$, the system has no periodic orbit.

If $(b, K) \in V_1^2$, by Theorem 4.4, system (1.3) undergoes a supercritical Hopf bifurcation when $\hat{d} = \hat{d}_+$ ($\lambda = H_M$). It follows from Proposition 6.8 that the Hopf bifurcation occurs after the transcritical bifurcation involving E_μ and E_K at $\hat{d} = \hat{d}_{\mu K}$. For $\hat{d} \in (\hat{d}_+, \hat{d}_M)$, $0 < H_M < \lambda < \frac{1}{\sqrt{a}} < \mu < K$. By part 1 of Theorem 6.3, system (1.3) has neither periodic orbits nor homoclinic loops and hence has the phase portrait D.

If $(b, K) \in V_1^3$, the sequence of bifurcations is the same as in V_1^2 except that the supercritical Hopf bifurcation occurs before the transcritical bifurcation involving E_μ and E_K. Hence by part 1 of Theorem 6.3, no homoclinic bifurcations can occur.

If $(b, K) \in V_1^4$, then $0 < K < \frac{1}{\sqrt{a}}$. For $\hat{d} \in (0, \hat{d}_M)$, $K < \mu$. In this case, the transcritical bifurcation involves E_λ and E_K and occurs when $\hat{d} = \hat{d}_{\lambda K}$. Note that since $\mu > K$, no homoclinic bifurcation can occur by part 1 of Theorem 6.6.   □

THEOREM 6.22. *Fix all parameters except $\hat{d} > 0$. For $(b, K) \in V_2$, when $\hat{d} > 0$ increases, the sequence of phase portraits occurring in the interior of each subregion is given in Table 6.5. In the table, moving from left to right as $\hat{d}$ increases, the phase portrait changes as a result of one of the following bifurcations:*

TABLE 6.5

Sequences of phase portraits for $(b, K) \in V_2$. In the three regions indicated by a †, above the line L, instead of a saddle-node bifurcation of limit cycles, there could be a degenerate bifurcation for $\hat{d} = 0$. In this case the sequence of phase portraits would begin with C instead of A. If more than one sequence is shown for a given region, it indicates that all of the sequences given are possible.

V_2^0	A	D	I			
	$(0, \hat{d}_{\mu K})$	$(\hat{d}_{\mu K}, \hat{d}_M)$	$(\hat{d}_M, \infty)$			
$V_2^{1\dagger}$	A	C	B	F	D	I
	$(0, \hat{d}_{sn})$	$(\hat{d}_{sn}, \hat{d}_-)$	$(\hat{d}_-, \hat{d}_{\mu K})$	$(\hat{d}_{\mu K}, \hat{d}_+)$	$(\hat{d}_+, \hat{d}_M)$	$(\hat{d}_M, \infty)$
$V_2^{2\dagger}$	A	C	B	A	D	I
	$(0, \hat{d}_{sn})$	$(\hat{d}_{sn}, \hat{d}_-)$	$(\hat{d}_-, \hat{d}_+)$	$(\hat{d}_+, \hat{d}_{\mu K})$	$(\hat{d}_{\mu K}, \hat{d}_M)$	$(\hat{d}_M, \infty)$
V_2^3	A	B	A	D	I	
	$(0, \hat{d}_-)$	$(\hat{d}_-, \hat{d}_+)$	$(\hat{d}_+, \hat{d}_{\mu K})$	$(\hat{d}_{\mu K}, \hat{d}_M)$	$(\hat{d}_M, \infty)$	
V_2^4	A	B	F	D	I	
	$(0, \hat{d}_-)$	$(\hat{d}_-, \hat{d}_{\mu K})$	$(\hat{d}_{\mu K}, \hat{d}_+)$	$(\hat{d}_+, \hat{d}_M)$	$(\hat{d}_M, \infty)$	
V_2^5	A	D	F	D	I	
	$(0, \hat{d}_{\mu K})$	$(\hat{d}_{\mu K}, d_-)$	$(\hat{d}_-, \hat{d}_+)$	$(\hat{d}_+, \hat{d}_M)$	$(\hat{d}_M, \infty)$	
	A	D	H	F	D	I
V_2^6	$(0, \hat{d}_{\mu K})$	$(\hat{d}_{\mu K}, d_{sn})$	$(\hat{d}_{sn}, \hat{d}_-)$	$(\hat{d}_-, \hat{d}_+)$	$(\hat{d}_+, \hat{d}_M)$	$(\hat{d}_M, \infty)$
	A	C	H	F	D	I
	$(0, \hat{d}_{sn})$	$(\hat{d}_{sn}, d_{\mu K})$	$(\hat{d}_{\mu K}, \hat{d}_-)$	$(\hat{d}_-, \hat{d}_+)$	$(\hat{d}_+, \hat{d}_M)$	$(\hat{d}_M, \infty)$
V_2^7	A	D	F	E	I	
	$(0, \hat{d}_{\mu K})$	$(\hat{d}_{\mu K}, \hat{d}_-)$	$(\hat{d}_-, \hat{d}_l)$	$(\hat{d}_l, \hat{d}_M)$	$(\hat{d}_M, \infty)$	
$V_2^{8a,b,c}$	A	D	H	F	E	I
	$(0, \hat{d}_{\mu K})$	$(\hat{d}_{\mu K}, \hat{d}_{sn})$	$(\hat{d}_{sn}, \hat{d}_-)$	$(\hat{d}_-, \hat{d}_l)$	$(\hat{d}_l, \hat{d}_M)$	$(\hat{d}_M, \infty)$
$V_2^{8b,c}$	A	C	H	F	E	I
	$(0, \hat{d}_{sn})$	$(\hat{d}_{sn}, \hat{d}_{\mu K})$	$(\hat{d}_{\mu K}, \hat{d}_-)$	$(\hat{d}_-, \hat{d}_l)$	$(\hat{d}_l, \hat{d}_M)$	$(\hat{d}_M, \infty)$
V_2^{8c}		C	H	F	E	I
		$(0, \hat{d}_{\mu K})$	$(\hat{d}_{\mu K}, \hat{d}_-)$	$(\hat{d}_-, \hat{d}_l)$	$(\hat{d}_l, \hat{d}_M)$	$(\hat{d}_M, \infty)$
$V_2^{9\dagger}$	A	C	B	F	E	I
	$(0, \hat{d}_{sn})$	$(\hat{d}_{sn}, \hat{d}_-)$	$(\hat{d}_-, \hat{d}_{\mu K})$	$(\hat{d}_{\mu K}, \hat{d}_l)$	$(\hat{d}_l, \hat{d}_M)$	$(\hat{d}_M, \infty)$
$V_2^{10a,b,c}$	A	D	H	G	E	I
	$(0, \hat{d}_{\mu K})$	$(\hat{d}_{\mu K}, \hat{d}_{sn})$	$(\hat{d}_{sn}, \hat{d}_l)$	$(\hat{d}_l, \hat{d}_-)$	$(\hat{d}_-, \hat{d}_M)$	$(\hat{d}_M, \infty)$
$V_2^{10b,c}$	A	C	H	G	E	I
	$(0, \hat{d}_{sn})$	$(\hat{d}_{sn}, \hat{d}_{\mu K})$	$(\hat{d}_{\mu K}, \hat{d}_l)$	$(\hat{d}_l, \hat{d}_-)$	$(\hat{d}_-, \hat{d}_M)$	$(\hat{d}_M, \infty)$
V_2^{10c}		C	H	G	E	I
		$(0, \hat{d}_{\mu K})$	$(\hat{d}_{\mu K}, \hat{d}_l)$	$(\hat{d}_l, \hat{d}_-)$	$(\hat{d}_-, \hat{d}_M)$	$(\hat{d}_M, \infty)$
V_2^{11}	A	D	G	E	I	
	$(0, \hat{d}_{\mu K})$	$(\hat{d}_{\mu K}, \hat{d}_l)$	$(\hat{d}_l, \hat{d}_-)$	$(\hat{d}_-, \hat{d}_M)$	$(\hat{d}_M, \infty)$	

- *the transcritical bifurcation involving E_μ and E_K that occurs at $\hat{d} = \hat{d}_{\mu K}$;*
- *the saddle-node bifurcation involving E_λ and E_μ that occurs at $\hat{d} = \hat{d}_M$;*
- *a Hopf bifurcation that occurs when $\hat{d} = \hat{d}_-$ or $\hat{d} = \hat{d}_+$;*
- *a homoclinic bifurcation that occurs when $\hat{d} = \hat{d}_l$;*
- *a saddle-node bifurcation of limit cycles that occurs when $\hat{d} = \hat{d}_{sn}$.*

For $(b, K) \in V_2^0$, the sequence is complete.

For $(b, K) \in V_2^2 \cup V_2^3$, the sequences are complete up to an even number of extra saddle-node bifurcations of limit cycles.

For $(b, K) \in V_2^1 \cup V_2^4 \cup V_2^5 \cup V_2^6 \cup V_2^7 \cup V_2^9$, the sequences are complete up to an even number of extra supercritical homoclinic bifurcations and an even number of extra saddle-node bifurcations of limit cycles.

For $(b, K) \in V_2^8 \cup V_2^{10} \cup V_2^{11}$, the sequences are complete up to saddle-node bifurcations of limit cycles and an even number of extra homoclinic bifurcations.

Proof. The region V_2 has 12 subregions V_2^i $(i = 0, 1, \ldots, 11)$.

1. For $(b, K) \in V_2^0$, $0 < \frac{1}{\sqrt{a}} < H_m < H_M < K$. It follows from Theorem 4.4 and Corollary 6.5 that system (1.3) does not undergo Hopf bifurcations and has neither periodic orbits nor homoclinic loops. The only bifurcations that can occur are a transcritical bifurcation involving E_μ and E_K at $\hat{d} = \hat{d}_{\mu K}$ and a saddle-node bifurcation involving E_λ and E_μ at $\hat{d} = \hat{d}_M$. The transcritical bifurcation must occur before the saddle-node bifurcation involving E_λ and E_μ.

2. For $(b, K) \in V_2^1 \cup V_2^2 \cup V_2^6$, $0 < H_m < H_M < \frac{1}{\sqrt{a}} < K$. It follows from Theorem 4.4 that there exist $\hat{d}_-$ and $\hat{d}_+$ $(\hat{d}_- < \hat{d}_+)$ such that when $\hat{d} = \hat{d}_-$, a subcritical Hopf bifurcation occurs at $(H_m, F(H_m))$, and when $\hat{d} = \hat{d}_+$, a supercritical Hopf bifurcation occurs at $(H_M, F(H_M))$.

For $(b, K) \in V_2^1$, by Proposition 6.9, the Hopf bifurcation at $(H_m, F(H_m))$ occurs before the transcritical bifurcation involving E_μ and E_K, i.e., $\hat{d}_- < \hat{d}_{\mu K} < \hat{d}_+$. For $\hat{d} \in (\hat{d}_+, \hat{d}_M)$, there are two equilibria, E_λ and E_μ, satisfying $H_M < \lambda < \frac{1}{\sqrt{a}} < \mu < K$. By Theorem 6.3, the system has neither periodic orbits nor homoclinic loops. The two equilibria E_λ and E_μ disappear through a saddle-node bifurcation when $\hat{d} = \hat{d}_M$. If (b, K) is below the line L, by Proposition 6.17, there exists a $\hat{d}_{sn} < \hat{d}_+$ such that the system undergoes a saddle-node bifurcation of limit cycles. If (b, K) is above the line L, by part 3 of Remark 6.19, this saddle node bifurcation of limit cycles may not occur; instead, two limit cycles bifurcate from $\hat{d} = 0$.

For $(b, K) \in V_2^2$, it follows from Proposition 6.9 that the only difference from the case when $(b, K) \in V_2^1$ is that the transcritical bifurcation involving E_μ and E_K occurs after the Hopf bifurcation at $\hat{d} = \hat{d}_+$.

For $(b, K) \in V_2^6$, it follows from Proposition 6.9 that the transcritical bifurcation involving E_μ and E_K occurs before both Hopf bifurcations. Since V_2^6 sits entirely below the line L, by Proposition 6.17, there must exist a $\hat{d}_{sn} \in (0, \hat{d}_-)$ such that system (1.3) undergoes a saddle-node bifurcation of limit cycles. From part 4 of Remark 6.19, it is not clear whether $\hat{d}_{sn} < \hat{d}_{\mu K}$ or $\hat{d}_{\mu K} < \hat{d}_{sn}$.

3. For $(b, K) \in V_2^3 \cup V_2^4 \cup V_2^5$, $0 < H_m < H_M < \frac{1}{\sqrt{a}} < K$. By Theorem 4.4, there are two supercritical Hopf bifurcations, the first at $\hat{d} = \hat{d}_-$ and the second at $\hat{d} = \hat{d}_+$.

It follows from Proposition 6.9 that if $(b, K) \in V_2^3$, $\hat{d}_- < \hat{d}_+ < \hat{d}_{\mu K}$; if $(b, K) \in V_2^4$, $\hat{d}_- < \hat{d}_{\mu K} < \hat{d}_+$; if $(b, K) \in V_2^5$, $\hat{d}_{\mu K} < \hat{d}_- < \hat{d}_+$.

4. For $(b, K) \in V_2^7$, $0 < H_m < \frac{1}{\sqrt{a}} < H_M < K$. By Theorem 4.4, there exists a $\hat{d}_- \in (0, \hat{d}_M)$ such that when $\hat{d} = \hat{d}_-$, system (1.3) undergoes a supercritical Hopf

F	E	F
$(\hat{d}_{\mu K}, \hat{d}_{l1})$	$(\hat{d}_{l1}, \hat{d}_{l2})$	$(\hat{d}_{l2}, \hat{d}_+)$

bifurcation. By Proposition 6.9, $\hat{d}_{\mu K} < \hat{d}_-$. By Theorem 6.7 and Lemma 6.10, there exists a $\hat{d}_l$ such that when $\hat{d} = \hat{d}_l$, the system undergoes a supercritical homoclinic bifurcation. The homoclinic bifurcation must destroy the periodic orbit created by the Hopf bifurcation, so $\hat{d}_l > \hat{d}_-$.

5. For $(b, K) \in V_2^8 \cup V_2^9 \cup V_2^{10} \cup V_2^{11}$, $0 < H_m < \frac{1}{\sqrt{a}} < H_M < K$. By Theorem 4.4, there exists a unique $\hat{d}_- \in (0, \hat{d}_M)$ such that when $\hat{d} = \hat{d}_-$, system (1.3) undergoes a subcritical Hopf bifurcation. Therefore, an unstable periodic orbit must exist when $\hat{d}_- - \epsilon < \hat{d} < \hat{d}_-$ for some ϵ. This periodic orbit must be created in either (i) a saddle-node bifurcation of limit cycles for some $\hat{d}_{sn} < \hat{d}_-$, or (ii) a degenerate bifurcation at $\hat{d} = 0$ creating an even number of limit cycles, or (iii) a subcritical homoclinic bifurcation. In cases (i) and (ii), the outside, asymptotically stable periodic orbit would have to be destroyed in a supercritical homoclinic bifurcation. Thus, in all three cases, there must exist a $\hat{d}_l$ at which a homoclinic bifurcation occurs.

By definition of $Dhom$, the homoclinic bifurcation changes stability and is subcritical in V_2^{11} and supercritical in $V_2^8 \cup V_2^9 \cup V_2^{10}$. By definition of HH, $\hat{d}_l < \hat{d}_-$ to the left of HH and $\hat{d}_l > \hat{d}_-$ to the right of HH. By definition of $E_{\mu K}$, $\hat{d}_- < \hat{d}_{\mu K}$ to the right of the branch of $E_{\mu K}$ with $b < 0$, and $\hat{d}_- > \hat{d}_{\mu K}$ to the left of this branch.
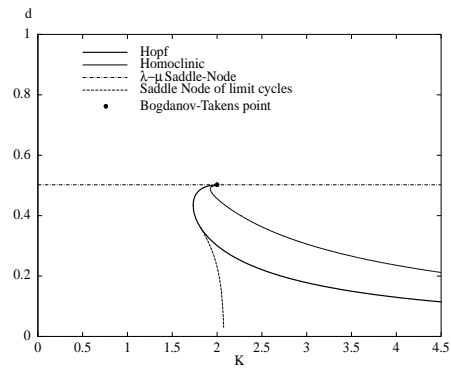
For $(b, K) \in V_2^{11}$, there is a subcritical homoclinic bifurcation at $\hat{d} = \hat{d}_l$ (i.e., case (iii) occurs) and by part 1 of Lemma 6.12, $\hat{d}_l < \hat{d}_-$. By part 1 of Theorem 6.6, $\hat{d}_{\mu K} < \hat{d}_l$. Therefore $0 < \hat{d}_{\mu K} < \hat{d}_l < \hat{d}_- < \hat{d}_M$.

For $(b, K) \in V_2^{10} \cup V_2^9 \cup V_2^8$, the homoclinic bifurcation is supercritical. In $V_2^{10a} \cup V_2^{10b} \cup V_2^{8a} \cup V_2^{8b}$ and V_2^9 below the line L case (i) occurs. In $V_2^{10c} \cup V_2^{8c}$ and V_2^9 above the line L, case (i) or (ii) occurs.
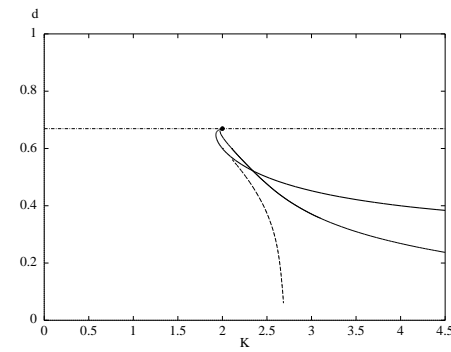
6. By part 1 of Theorem 6.6 and part 1 of Theorem 6.3, there is no homoclinic bifurcation for $(b, K) \in V_2^2 \cup V_2^3$. Solutions are bounded. There are either an even number or zero limit cycles for $\hat{d} > 0$ sufficiently small, and there are no limit cycles for $\hat{d} > \hat{d}_M$. We have considered all the other possible local and necessary global bifurcations. Hence, the sequences are complete as described in Table 6.5 up to saddle-node bifurcations of limit cycles and homoclinic bifurcations as indicated in the statement of the theorem.   ☐

Remark 6.23. The sequence of phase portraits in Table 6.5 is complete up to saddle-node bifurcations of limit cycles and homoclinic loop bifurcations. For $(b, K) \in V_2^1$ and $\hat{d} \in (\hat{d}_{\mu K}, \hat{d}_+)$, numerical simulations using XPPAUT [11] suggest that in addition to the critical values shown in the table, there could exist $\hat{d}_{l1}, \hat{d}_{l2} \in (\hat{d}_{\mu K}, \hat{d}_+)$ such that when $\hat{d} = \hat{d}_{l1}$ and $\hat{d} = \hat{d}_{l2}$, system (1.3) undergoes homoclinic bifurcations and includes the subsequence of phase portraits listed in Table 6.6.
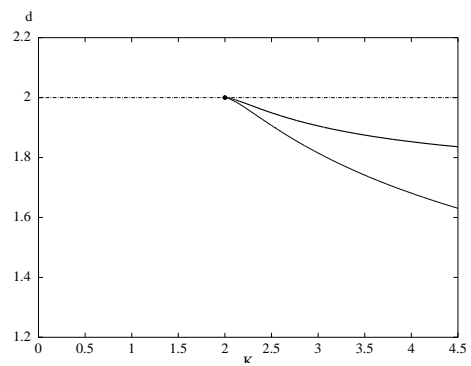
Numerical continuation of bifurcation curves carried out with the software Auto (through the XPPAUT [11] interface), supports our analysis. Fixing $a = m = c = r = 1$, which is consistent with the rescaling (1.7), we calculated the two parameter bifurcation sets in dK space, for $b = 0, -0.5, -1.5$ (Figure 6.5). Fixing K in Figure 6.5 and allowing d to vary vertically, we obtain sequences of bifurcations indicated by our analysis.

(a) $b = 0$

(b) $b = -0.5$

(c) $b = -1.5$

FIG. 6.5. *Two dimensional bifurcation diagram from XPPAUT* [11]: $a = m = c = r = 1$.

7. Discussion. This study was stimulated by a series of papers [13, 19, 24]. In [24], six mechanisms for periodically forcing the classical predator-prey model with Holling type II response functions were shown, surprisingly, to have topologically equivalent 2-parameter bifurcation diagrams for the associated first return map with respect to fold, flip, and Neimark–Sacker bifurcation curves of the first and second iterates and period doubling cascades. Even more unexpectedly, in [13] it was shown that the eight mechanisms for periodically forcing the analogous predator-prey model in a chemostat not only produced topologically equivalent diagrams, but these diagrams were topologically equivalent to the ones for the classical model. They conjectured a "universal diagram" for forced predator-prey systems. In [24] the authors state explicitly that it would be of interest to extend their analysis to a predator-prey model that has saddle-node bifurcations of limit cycles and homoclinic bifurcations for the unforced system. System (1.3) seemed like an ideal choice, since we were aware from previous studies [12, 30, 25, 26, 28] that it had the indicated bifurcations as the carrying capacity was varied. We felt certain that it should be possible to obtain 2-parameter bifurcation diagrams of the periodically forced version of system (1.3) that were not topologically equivalent to the ones in [13] and [24].

To our surprise, when the carrying capacity was forced, the 2-parameter bifurcation diagram was not significantly different [32]. In order to find parameters that would produce different diagrams, it was necessary to perform a more detailed bifurcation analysis on the unforced system, i.e., system (1.3), in order to understand the role of all of the parameters, and this was the motivation for this paper.

In fact, based on the results in this paper, in [32], we are able to show that for the Holling type IV response functions, different mechanisms for periodic forcing result in topologically distinct 2-parameter bifurcation diagrams and hence can be different than the postulated universal diagram.

Our work in this paper, analyzing local and global bifurcations of system (1.3), extends and complements the work in [12, 30, 25, 26, 28]. We now understand the role of perturbing each of the parameters on the dynamics. We described, for any fixed $a > 0$, $-2\sqrt{a} < b$, and $K > 0$, the sequence of bifurcations and associated phase portraits which occur as $\frac{d}{cm} > 0$ is varied. These results are summarized in Figure 6.1 and Tables 6.1–6.5 and include both local and global bifurcations. In particular, explicit regions in parameter space are provided for all of the phase portraits illustrated in Table 6.2, including regions where there are at least two limit cycles. We showed that for any $a, r > 0$ and $-2\sqrt{a} < b$ there is a Bogdanov–Takens bifurcation of codimension 2 when $d = \frac{cm}{b+2\sqrt{a}}$ and $K = \frac{2}{\sqrt{a}}$ with $b \neq -\sqrt{a}$ and a Bogdanov–Takens bifurcation of codimension 3 when $b = -\sqrt{a}$, $d = \frac{cm}{\sqrt{a}}$, and $K = \frac{2}{\sqrt{a}}$. We proved that the parameters b, d, K give a versal unfolding of the codimension 3 bifurcation.

Although the model (1.3) contains seven parameters, our analysis shows that the parameter r has no effect on the existence and stability of equilibria, or of limit cycles created by Hopf bifurcations. Further, as seen in the results above, the parameters c, d, and m always occur in the ratio $\frac{d}{cm}$, and the parameter a acts as a scaling factor for b and K. These latter relations are not surprising given that a, c, and m could be removed via the rescaling (1.7), but these relations seem to indicate that this is the most "natural" way to reduce the seven parameters to four.

As discussed above, variation of the parameter d, the death rate of the predator, results in many different bifurcation sequences depending on the values of the other parameters. However, there is a common theme to all the sequences. For $d > 0$ small enough, any system starting with positive initial conditions will lead to coexistence of

the predator and the prey. For d large enough (i.e., $d > \frac{mc}{b+2\sqrt{a}}$), all initial conditions will result in extinction of the predator. In between there exists a range of values of d for which either coexistence or extinction of the predator can occur depending on the initial conditions. Most notably, if the initial prey population is large enough, then extinction of the predator will result regardless of the initial size of the predator population.

Our analysis allows us to describe the tremendous variation in the bifurcation sequences. In particular, we have shown that the coexistence of the predator and the prey can be in the form of a steady state or periodic solution, or, for some sets of parameters, both. We have not been able to exclude the possibility of further variation due to limit cycles appearing and disappearing in global bifurcations. Such variations can lead to biologically interesting sequences of bifurcations. One example, which we have observed numerically, discussed and listed in Table 6.6, involves two homoclinic bifurcations that occur in succession as d is increased. The result is that the system goes from a state where coexistence is possible to one where it is not and then back again. This gives rise to the surprising result that, for this set of parameters, *increasing* the per capita death rate of the predator actually *increases* the predator population's chance of survival (or analogously, *reducing* the per capita death rate of the predator *reduces* the predator population's chances of survival).

REFERENCES

[1] J. F. ANDREWS, *A mathematical model for the continuous culture of microorganisms utilizing inhibitory substrates*, Biotechnol. Bioeng., 10 (1968), pp. 707–723.

[2] A. ANDRONOV, E. LEONTOVICH, I. GORDON, AND A. MAIER, *Theory of Bifurcations of Dynamical Systems on a Plane*, Israel Program for Scientific Translations, Halstead Press, Jerusalem, 1971.

[3] A. D. BAZYKIN, *Nonlinear Dynamics of Interacting Populations*, World Sci. Ser. Nonlinear Sci. Ser. A Monogr. Treatises 11, World Scientific, River Edge, NJ, 1998.

[4] K.-S. CHENG, *Uniqueness of a limit cycle for a predator-prey system*, SIAM J. Math. Anal., 12 (1981), pp. 541–548.

[5] S. N. CHOW AND J. K. HALE, *Methods of Bifurcation Theory*, Grundlehren Math. Wiss. 251, Springer–Verlag, New York-Berlin, 1982.

[6] F. DUMORTIER, *Singularities of Vector Fields*, Monogr. Mat. 32, Instituto de Matemática Pura e Aplicada, Rio de Janeiro, 1978.

[7] F. DUMORTIER AND R. ROUSSARIE, *Étude locale des champs de vecteurs à paramètres*, in Journées Singuliéres de Dijon (Univ. Dijon, Dijon, 1978), Astérisque 59–60, Soc. Math. France, Paris, 1978, pp. 3, 7–42 (in French).

[8] F. DUMORTIER, R. ROUSSARIE, AND J. SOTOMAYOR, *Generic 3-parameter families of vector fields on the plane, unfolding a singularity with nilpotent linear part. The cusp case of codimension 3*, Ergodic Theory Dynam. Systems, 7 (1987), pp. 375–413.

[9] F. DUMORTIER, R. ROUSSARIE, AND C. ROUSSEAU, *Hilbert's 16th problem for quadratic vector fields*, J. Differential Equations, 110 (1994), pp. 86–133.

[10] F. DUMORTIER, R. ROUSSARIE, J. SOTOMAYOR, AND H. ŻOLADEK, *Bifurcations of Planar Vector Fields. Nilpotent Singularities and Abelian Integrals*, Lecture Notes in Math. 1480, Springer–Verlag, Berlin, 1991.

[11] B. ERMENTROUT, *Simulating, Analyzing, and Animating Dynamical Systems: A guide to XPPAUT for researchers and students*, SIAM, Philadelphia, 2002.

[12] H. I. FREEDMAN AND G. S. K. WOLKOWICZ, *Predator-prey systems with group defence: The paradox of enrichment revisited*, Bull. Math. Biol., 48 (1986), pp. 493–508.

[13] A. GRAGNANI AND S. RINALDI, *A universal bifurcation diagram for seasonally perturbed predator-prey models*, Bull. Math. Biol., 57 (1995), pp. 701–712.

[14] C. S. HOLLING, *The components of predation as revealed by a study of small-mammal predation of the European pine sawfly*, Can. Entomol., 91 (1959), pp. 293–320.

[15] C. S. HOLLING, *The functional response of predators to prey density and its role in mimicry and population regulation*, Mem. Entomolog. Soc. Canada, 45 (1965), pp. 3–60.

[16] N. KASARINOFF AND P. VAN DER DEIESCH, *A model of predator-prey system with functional response*, Math. Biosci., 39 (1978), pp. 124–134.

[17] M. KOT, *Elements of Mathematical Ecology*, Cambridge University Press, Cambridge, UK, 2001.

[18] Y. A. KUZNETSOV, *Elements of Applied Bifurcation Theory*, Appl. Math. Sci. 112, Springer–Verlag, New York, 1995.

[19] Y. A. KUZNETSOV, S. MURATORI, AND S. RINALDI, *Bifurcations and chaos in a periodic predator-prey model*, Internat. J. Bifur. Chaos Appl. Sci. Engrg., 2 (1992), pp. 117–128.

[20] Y. A. KUZNETSOV, *CONTENT-Integrated Environment for Analysis of Dynamical Systems*, Report UPMA-98-224, Ecole Normale Supericure de Lyon, Lyon, France, 1998.

[21] P. MARDĚSIĆ, *Chebyshev Systems and the Versal Unfolding of the Cusps of Order n*, Travaux en Cours 57, Hermann, Paris, 1998.

[22] J. E. MARSDEN AND M. MCCRACKEN, *The Hopf Bifurcation and Its Applications*, Appl. Math. Sci. 19, Springer–Verlag, New York, 1976.

[23] A. MOURTADA, *Cyclicité finie des polycycles hyperboliques de champs de vecteurs du plan: mise sous forme normale*, in Bifurcations of Planar Vector Fields (Luminy, 1989), Lecture Notes in Math. 1455, Springer–Verlag, Berlin, 1990, pp. 272–314.

[24] S. RINALDI, S. MURATORI, AND Y. A. KUZNETSOV, *Multiple attractors, catastrophes and chaos in seasonally perturbed predator-prey communities*, Bull. Math. Biol., 55 (1993), pp. 15–35.

[25] F. ROTHE AND D. S. SHAFER, *Bifurcation in a quartic polynomial system arising in biology*, in Bifurcations of Planar Vector Fields (Luminy, 1989), Lecture Notes in Math. 1455, Springer–Verlag, Berlin, 1990, pp. 356–368.

[26] F. ROTHE AND D. S. SHAFER, *Multiple bifurcation in a predator-prey system with nonmonotonic predator response*, Proc. Roy. Soc. Edinburgh Sect. A, 120 (1992), pp. 313–347.

[27] R. ROUSSARIE, *A note on finite cyclicity property and Hilbert's* 16*th problem*, in Dynamical Systems, Valparaiso 1986, Lecture Notes in Math. 1331, Springer–Verlag, Berlin-New York, 1988, pp. 161–168

[28] S. RUAN AND D. XIAO, *Global analysis in a predator-prey system with nonmonotonic functional response*, SIAM J. Appl. Math., 61 (2001), pp. 1445–1472.

[29] *Waterloo Maple Software* V, University of Waterloo, Waterloo, Canada, 1990.

[30] G. S. K. WOLKOWICZ, *Bifurcation analysis of a predator-prey system involving group defence*, SIAM J. Appl. Math., 48 (1988), pp. 592–606.

[31] D. WRZOSEK, *Limit cycles in predator-prey models*, Math. Biosci., 98 (1990), pp. 1–12.

[32] H. ZHU, S. A. CAMPBELL, AND G. S. WOLKOWICZ, *Seasonal Forcing of a Predator-Prey Model with Nonmonotonic Functional Response*, in preparation.